



Aalborg Universitet

AALBORG UNIVERSITY
DENMARK

Point pattern simulation modelling of extensive and intensive chicken farming in Thailand

Accounting for clustering and landscape characteristics

Chaiban, Celia; Biscio, Christophe; Thanapongtharm, Weerapong; Tildesley, Michael J. ; Xiao, Xiangming ; Robinson, Timothy P. ; Vanwambeke, Sophie O.; Gilbert, Marius

Published in:
Agricultural Systems

DOI (link to publication from Publisher):
[10.1016/j.agry.2019.03.004](https://doi.org/10.1016/j.agry.2019.03.004)

Creative Commons License
CC BY-NC-ND 4.0

Publication date:
2019

Document Version
Accepted author manuscript, peer reviewed version

[Link to publication from Aalborg University](#)

Citation for published version (APA):

Chaiban, C., Biscio, C., Thanapongtharm, W., Tildesley, M. J., Xiao, X., Robinson, T. P., Vanwambeke, S. O., & Gilbert, M. (2019). Point pattern simulation modelling of extensive and intensive chicken farming in Thailand: Accounting for clustering and landscape characteristics. *Agricultural Systems*, 173, 335-344. <https://doi.org/10.1016/j.agry.2019.03.004>

General rights

Copyright and moral rights for the publications made accessible in the public portal are retained by the authors and/or other copyright owners and it is a condition of accessing publications that users recognise and abide by the legal requirements associated with these rights.

- Users may download and print one copy of any publication from the public portal for the purpose of private study or research.
- You may not further distribute the material or use it for any profit-making activity or commercial gain
- You may freely distribute the URL identifying the publication in the public portal -

Take down policy

If you believe that this document breaches copyright please contact us at vbn@aub.aau.dk providing details, and we will remove access to the work immediately and investigate your claim.

1 **Point pattern simulation modelling of extensive and intensive chicken farming**
2 **in Thailand: accounting for clustering and landscape characteristics.**

3

4 Celia Chaiban^{1,2}, Christophe Biscio³, Weerapong Thanapongtharm⁴, Michael Tildesley⁵,
5 Xiangming Xiao⁶, Timothy P Robinson⁷, Sophie O Vanwambeke^{1,*}, Marius Gilbert^{2,8,*}.

6

7 ¹ Georges Lemaître Centre for Earth and Climate research, Earth and Life Institute, Université catholique
8 de Louvain, Louvain-la-Neuve, Belgium.

9 ² Spatial Epidemiology Lab. (SpELL), Université Libre de Bruxelles, Brussels, Belgium.

10 ³ Department of Mathematical Sciences, Aalborg University, Denmark

11 ⁴ Department of Livestock Development (DLD), Bangkok 10400, Thailand.

12 ⁵ School of Life Sciences and Mathematics Institute, University of Warwick, Warwick, UK

13 ⁶ Department of Microbiology and Plant Biology, Center for Spatial Analysis, University of Oklahoma,
14 Norman, Oklahoma, USA.

15 ⁷ Livestock Information, Sector Analysis and Policy Branch (AGAL), Food and Agriculture Organization
16 of the United Nations (FAO), Viale delle Terme di Caracalla, 00153 Rome, Italy.

17 ⁸ Fonds National de la Recherche Scientifique (FNRS), Brussels, Belgium.

18

19 * corresponding authors SVW (sophie.vanwambeke@uclouvain.be) and MG (mgilbert@ulb.ac.be)

20

21

22 **Abstract**

23 In recent decades, intensification of animal production has been occurring rapidly in transition
24 economies to meet the growing demands of increasingly urban populations. This comes with
25 significant environmental, health and social impacts. To assess these impacts, detailed maps
26 of livestock distributions have been developed by downscaling census data at the pixel level
27 (10km or 1km), providing estimates of the density of animals in each pixel. However, these
28 data remain at fairly coarse scale and many epidemiological or environmental science
29 applications would make better use of data where the distribution and size of farms are
30 predicted rather than the number of animals per pixel. Based on detailed 2010 census data,
31 we investigated the spatial point pattern distribution of extensive and intensive chicken farms
32 in Thailand. We parameterized point pattern simulation models for extensive and intensive
33 chicken farms and evaluated these models in different parts of Thailand for their capacity to
34 reproduce the correct level of spatial clustering and the most likely locations of the farm
35 clusters. We found that both the level of clustering and location of clusters could be simulated
36 with reasonable accuracy by our farm distribution models. Furthermore, intensive chicken
37 farms tended to be much more clustered than extensive farms, and their locations less easily
38 predicted using simple spatial factors such as human populations. These point-pattern
39 simulation models could be used to downscale coarse administrative level livestock census
40 data into farm locations. This methodology could be of particular value in countries where farm
41 location data are unavailable.

42

43 **Keywords**

44 Agricultural intensification, Point pattern analysis, Farm distribution model, Livestock
45 production systems

46

47 **1. Introduction**

48 Following demographic and economic development, the per capita consumption of animal-
49 source food has increased continuously over the past few decades, with significant
50 consequences for livestock production (Delgado, 1999; Slingenbergh et al., 2013; Steinfeld,
51 2004). The growth in demand for animal products, mainly meat, eggs and milk, was met
52 primarily through intensification of livestock production, which was particularly marked for
53 monogastric species such as poultry and pigs (Gilbert et al., 2015; Smil, 2002). Interest in good
54 spatial data on livestock distribution has grown along intensification and the growing
55 importance of livestock as a food and income source, as well as a source of environmental
56 and sanitary issues (Burdett et al., 2015; Martin et al., 2015; Steinfeld et al., 2006). Several
57 challenges exist in relation to the production of such maps, among which the level of
58 intensification and the available source data stand out.

59

60 In most high-income countries, detailed farm registers exist, but are often distributed in
61 aggregated form to protect privacy. In low and middle-income countries, registers rarely exist
62 and the most accurate data sets are produced through agricultural censuses, the detail of
63 which varies considerably across countries (Robinson et al., 2014; Wint et al., 2007). Both
64 situations, from data-rich or -poor countries, may lead to livestock statistics being only available
65 at coarse spatial scales insufficient for detailed analyses. To increase the spatial detail of
66 coarse livestock data, previous studies on livestock distribution mapping developed spatial
67 statistical algorithms linking densities to environmental variables to downscale census data
68 from administrative boundaries to density estimates at the pixel level. This represents livestock
69 densities varying gradually across pixels, as in databases such as the Gridded Livestock of
70 the World (GLW) version 1 (Wint et al., 2007), version 2 (Robinson et al., 2014) and version 3
71 (Gilbert et al., In press). Other authors have applied similar approaches to map livestock at
72 country or continental scale (Neumann et al., 2009; Prosser et al., 2011; Van Boeckel et al.,
73 2011).

74

75 In addition to a lack of spatial detail, a distinction between intensive and extensive production
76 systems, is rarely made. Intensive systems were defined as large-scale commercial, market-
77 oriented and high-input farms and extensive systems as small-scale, low-input backyard
78 production systems (Van Boeckel et al., 2012). However, this is an important distinction in
79 terms of their health and environmental impacts (Van Boeckel et al., 2012; Gerber et al., 2013;
80 Jones et al., 2013a; Gilbert et al., 2015). More specifically, intensification of pig and poultry
81 production comes with significant, among others, health impacts (Leibler et al., 2009; Mennerat
82 et al., 2010; Pulliam et al., 2012; Jones et al., 2013b; Slingenbergh et al., 2013; Van Boeckel
83 et al., 2014). Health impacts, notably through pathogen emergence and re-emergence, has a
84 potential global relevance, as illustrated by the threat of pandemic influenza (Leibler et al.,
85 2009; Li et al., 2004; Monne et al., 2014). Intensified systems promote high densities of
86 genetically similar individuals, which promotes pathogen amplification, selection of more
87 virulent pathogens and risk of pathogen spill-over (Jones et al., 2013a). Owing to their close
88 interactions with humans, particularly in peri-urban environments, and possible contacts with
89 wild animals, intensive production systems can also serve as an intermediate between wildlife
90 and human populations and as amplifier (Childs et al., 2007). Differentiating between extensive
91 and intensive systems, or simply knowing where the largest farms are, is therefore particularly
92 important in regions where production is currently undergoing intensification, as the
93 distributions of extensive and intensive farms may have different spatial patterns and may
94 change rapidly through time. Thus far, few attempts have been made to distinguish extensive
95 from intensive production systems. Gilbert et al. (2015) developed an approach to separate
96 extensive from intensively raised animals in global chicken and pig maps based on a simple
97 mode using GDP per capita. At the country scale, Van Boeckel *et al.* (2012) observed a distinct
98 bimodal distribution in poultry farms in Thailand that could be used to distinguish extensive
99 from intensive farms. They modelled extensive and intensive poultry separately using a
100 methodology similar to that of GLW, and noted a relatively poor predictive accuracy for
101 intensively-raised chickens compared to extensive chickens using that approach.

102

103 Finally, a continuous surface, pixel-based model may not be the best way to represent
104 intensive farms. Indeed, intensification of poultry production is such that a very large number
105 of birds can be present in a single location (e.g. typically more than 100 000 birds can be found
106 in a farm or site), with very few in an adjacent pixel. A discrete spatial representation of
107 individual farms as single point locations, with the number of birds as an attribute, may thus
108 represent intensive farms better than a continuous surface image. Another issue with regards
109 to modelling farm locations instead of animal densities is that such models would better fit the
110 needs of mathematical models of livestock diseases (Martin et al., 2015). Epidemic
111 mathematical transmission models may be sensitive to the spatial clustering, distribution, type
112 and overall density of farms (Reeves, 2012; Tildesley and Ryan, 2012), and mitigation
113 measures of disease transmission are in part based on the distance between farms. Fine-scale
114 maps of farm distribution, including farm position and level of clustering, could thus make an
115 important contribution to models that can inform control strategies (Bruhn et al., 2012). While
116 broad-scale clusters of farms may be captured by aggregated data, the factors influencing
117 farm distribution are poorly known at finer scales (Burdett et al., 2015). In the presence of
118 aggregated census data, the distribution of individual farm locations have tended to be based
119 on random allocation of points, regardless of other geographic information (Tildesley et al.,
120 2010) or, in some cases, constrained by geographical information contained in probability
121 surfaces (Bruhn et al., 2012; Burdett et al., 2015; Emelyanova et al., 2009; Tildesley and Ryan,
122 2012). However, none of these methods have captured both the number of points and the
123 pairwise interaction between points (first and second order characteristics) to predict the
124 spatial clustering of farms as well as differences in their broader distributions.

125

126 In this paper, we investigated the use of point-pattern models as a way to predict the
127 distribution of individual farms both in terms of spatial clustering and in terms of dependency
128 on external variables influencing their presence. This approach may provide more realistic
129 representations of animal distribution at fine spatial scales than continuous pixel-based
130 distributions, especially for species such as poultry and pigs that may be raised in high

131 numbers in single premises. Our analyses focused on Thailand chicken farms, as an example
132 of a middle-income country where extensive production systems (backyard poultry farms)
133 coexist with intensive ones (large-scale chicken farms) (Van Boeckel et al., 2012).

134

135 **2. Methods**

136 *2.1. Data*

137 A detailed census of poultry holders was conducted in 2010 by the Department of Livestock
138 Development (DLD), Bangkok, Thailand. The census included the number of chickens per
139 owner for all farms in Thailand. The administrative levels in Thailand are province, district, sub-
140 district and village, the latter being the smallest. The three first levels have defined boundaries,
141 while villages are recorded by coordinates, usually at the center of the main cluster of houses.
142 During the census, the coordinates of each poultry holder were not collected. The coordinates
143 of the village were subsequently linked to each poultry holder. The census recorded 1,936,590
144 chicken owners in a total of 62,091 villages. Henceforth, we will use the term 'farm' to represent
145 both smallholders, who may be a single family with a few chickens, and large-scale farms
146 having several thousand birds. Farms with no chickens were removed from the dataset. A set
147 of Voronoi polygons (Okabe et al., 2000) was built from the village coordinates. The median
148 area of the Voronoi polygons was 4 km², the mean area was 8 km² (Supplementary Material
149 (SM) – Figure S1). A mask excluding permanent water bodies and the province and city of
150 Bangkok was applied. Individual farms were assigned a random coordinate within their polygon
151 excluding of masked areas. Our input data set thus did not include the exact locations of farms,
152 but an approximate location. However, given the extent (whole of Thailand) and the resolution
153 of our predictors (1km), we considered this loss of accuracy to have a negligible effect on our
154 results.

155

156 The distribution of chickens per farm showed a clear bimodal pattern (Van Boeckel et al., 2012)
157 and a threshold of 500 chickens per farm was used to separate extensive small-scale
158 producers from intensive large-scale systems. This threshold maximized the correlation

159 between the quantiles of the intensive and extensive distributions of animals per farm in the
 160 two groups and the quantiles of two normal distributions of same mean and standard deviation.
 161 This resulted in two datasets of 1,930,003 extensive farms with a median number of 20
 162 chickens per farm, and 6,587 intensive farms with a median number of 8,000 chickens per
 163 farm. In the absence of other information on the farm (size, inputs, outputs, practices), we
 164 assumed flock size to be an acceptable proxy for the classification in ‘extensive’ or ‘intensive’
 165 holdings.

166
 167 Spatial predictor variables were selected to be both generic and available in databases with a
 168 global extent (Table 1, Fig. 1) so that the models and approaches followed in this study could
 169 be transferred to data-poor countries. The predictor variables were previously identified as
 170 having strong predictive capacity by Van Boeckel (2012). The logarithm (base 10) of human
 171 population density (Worldpop database, <http://www.worldpop.org.uk> was included as farms
 172 are unlikely to be located either in city centres or in completely remote areas. “Remoteness”,
 173 defined as the travel time to Bangkok and to the closest provincial capital, accounted for
 174 differences in accessibility to provincial or national markets through the road and railway
 175 networks. This was computed from Nelson’s accessibility which is based on a cost-distance
 176 algorithm in unit of time. The weighted surface accounts for transport networks, environment
 177 and political factors affecting travel times (Nelson, 2008). Thus, it also helps identifying areas
 178 less suitable for chicken farms. Tree cover or percentage of land covered by forest was
 179 included as areas covered by dense and permanent forest may also exclude poultry farming
 180 (Hansen et al., 2013). Cropland or percentage of land covered by crops accounted for areas
 181 providing access to grain for feed (Fritz et al., 2015).

182

183 **Table 1. Predictor variables tested in our models**

	<i>Resolution (m)</i>	<i>Units</i>	<i>Reference</i>
<i>Human population density</i>	1000	People per km ²	Worldpop database
<i>Remoteness</i>	1000	Minute	Nelson et al. 2008

<i>Cropland</i>	1000	Pixel % covered by crops	Fritz et al. 2015
<i>Tree cover</i>	1000	Pixel % covered by forest	Hansen et al. 2013

184

185 2.2. Sample areas

186 The analysis was applied on squares samples of equal area sampling the Thai territory (Fig.
 187 2). This allowed keeping processing time reasonable by dealing with a fraction of the very
 188 numerous chicken farms in Thailand and also avoided computational difficulties at the complex
 189 edges of the country. Creating sample areas also allowed to cross-validate model results. The
 190 size and location of the sample areas were chosen to cover most of Thailand completely, to
 191 cover a sufficient number of farms, and to include a diversity of predictor values and farm
 192 densities. For intensive farms, Thailand was divided into square areas of 200 x 200 km, and
 193 we analysed only the 11 sample areas with over 250 farms (Fig. 2a). For extensive farms, 38
 194 sample areas of 112 x 112 km, each having at least half over Thailand, were used (Fig. 2b).

195

196 2.3. Descriptive analysis

197 The distribution of extensive and intensive farm locations was investigated using point pattern
 198 analysis. We used the stationary and non-stationary Besag's L-function, a transformation of
 199 Ripley's K-function, to define the spatial pattern of intensive and extensive farms between three
 200 different broad types of point pattern: random, clustered and regular. The random case referred
 201 to the completely spatial randomness (CSR) or homogenous Poisson process model. The L-
 202 functions were estimated by sample areas with *Lest()* and *Linhom()* functions from the *spastat*
 203 package in R.

204

205 Ripley's K-function is a summary statistic of a point process, defined as the expected number
 206 of r -neighbours of a point of \mathbf{X} divided by the intensity λ i.e.:

$$207 \quad K(r) = \frac{1}{\lambda} \mathbb{E}[\text{number of neighbours of } u \mid \mathbf{X} \text{ has a point at location } u]$$

208 for any $r \geq 0$ at any location u , where r is the radius, λ is the homogeneous intensity of points,
 209 \mathbf{X} is the point process and u is any location. This definition assumes that the process is

210 stationary, which imply that the intensity is constant and does not depend on the location
 211 (Baddeley et al., 2015). The empirical K-function is a summary of the pairwise distances of a
 212 point pattern, which allows point patterns with different intensities to be compared, and the
 213 analysis of a pattern at different scales, since the function is normalized by the intensity. The
 214 empirical K-function is defined as

$$215 \quad \hat{K}(r) = \left(\frac{a}{n(n-1)} \right) \sum_{i,j=1; i \neq j} I(d[i,j] \leq r) e[i,j]$$

216 where a is the study area, n is the total number of points in a , the sum is taken over all ordered
 217 pairs of distinct points i and j , $d[i,j]$ is the distance between two points and $I(d[i,j] \leq r)$ is the
 218 indicator that equals 1 if the distance is less than or equal to r . The term $e[i,j]$ is the edge
 219 correction weight, which was discarded as the number of points considered in both datasets
 220 was very large. By using $\frac{a}{n(n-1)}$, it assumes that the process is stationary. An observed point
 221 pattern is considered as clustered, random or regular depending on whether its empirical K-
 222 function is respectively higher than, close to or lower than the K-function of a CSR, i.e. the
 223 curve of equation $y = \pi r^2$. In the case of a non-stationary process, a generalisation of the later
 224 should be used, the inhomogeneous K-function. This generalisation assumes that \mathbf{X} is a point
 225 process with a non-constant intensity $\lambda(u)$ at each location u , i.e.

$$226 \quad \hat{K}_{inhom}(r) = \left(\frac{1}{A} \right) \sum_i \sum_{j, i \neq j} \frac{1(d[i,j] \leq r)}{(\lambda(x_i)\lambda(x_j))}$$

227 where A is a constant denominator, and $d[i,j]$ is the distance between points x_i and x_j (Baddeley
 228 et al., 2000). Besag's L-function $L(r) = \sqrt{\frac{K(r)}{\pi}}$ is a transformation of the K-function for which a
 229 CSR is a straight line $L_{random}(r) = r$ when $L(r)$ is plotted against r .

230

231 2.4. Point pattern simulation

232 2.4.1. Model choice

233 To predict the spatial distribution of intensive and extensive farms as points, the Log-Gaussian
 234 Cox Processes (LGCP) model was used (Møller et al., 1998), with the Palm maximum

235 likelihood method of parameter optimisation (Baddeley et al., 2015; Tanaka et al., 2008). The
236 Palm maximum likelihood method provides almost the same results as the minimum contrast
237 method and our study may be done with both of these algorithm (Baddeley et al., 2015).

238

239 We compared the five processes modelling clustered point patterns; the Matérn cluster
240 process, the Thomas process, the Cauchy cluster process, the Variance gamma cluster
241 process and the LGCP with exponential covariance function (SM-Figure S 2) (Baddeley et al.,
242 2015). These models were fitted on one sample area of 200 km length in Thailand using the
243 intensive dataset, including covariates with the command line `kppm(X, ~ Hpop + Crop + Tree`
244 `+ Remot + I(Hpop^2)+ I(Crop^2) + I(Tree^2) + I(Remot^2), clusters =`
245 `c("Thomas","MatClust","Cauchy","VarGamma","LGCP"), method = "palm")` using the `kppm()`
246 function from `spatstat` package in R (all other arguments had default settings). The covariates
247 were selected based on the Akaike Information Criterion (AIC) as below. We assessed how
248 these different models were able to reproduce the clustering of the observed point pattern by
249 using the two-sided global rank envelope test. The hypothesis tested by the rank envelope test
250 is that the model tested can explain the process from which the observed point pattern
251 originates. The test provides a p-value and a graphical representation of the envelope. The p-
252 value decreases when the empirical L-function goes out of the global rank envelope. It was
253 implemented based on extreme rank lengths with the `global_rank_envelope()` function from
254 `GET` package in R (Mrkvička et al., 2017; Myllymäki et al., 2017) for 100,000 simulations of
255 each model. The extreme rank lengths type was selected because it allowed to run fewer
256 simulations (Mrkvička et al., 2016; Myllymäki et al., 2017). The conclusion of the extreme rank
257 envelope test was that the LGCP performed best. It had by far the highest p-value, 5.40e-02,
258 compared to the other models with a p-value of 2.80e-04, 2.40e-04, 1.08e-03, 6.48e-03, for
259 the Matern, Thomas, Variance Gamma, Cauchy models, respectively (SM – Figure S 3).
260 Hence, LGCP was used for all subsequent modelling of clustered point patterns.

261

262 *2.4.2. Model fitting and validation*

263 Four different types of model were built and compared: (i) “CSR”: a completely spatial
 264 randomness (CSR) or homogenous Poisson process model, which randomly distributed farms;
 265 (ii) “iCSR”: inhomogeneous Poisson process model, a CSR in which the average density of
 266 points is spatially varying. The average density is an intensity function $\lambda(u)$ of spatial location
 267 u . In our model, the intensity was modelled as $\lambda = \exp(\text{covariates})$; (iii) “LGCP”: a LGCP
 268 model with a homogeneous intensity (without any covariates) with an exponential covariance
 269 function (Baddeley et al., 2015); and (iv) “iLGCP”: a LGCP model with covariates predicting
 270 an inhomogeneous intensity and identifying highly probable locations for clusters. iLGCP was
 271 defined with a covariate exponential function and a random intensity modelled as $\lambda = \exp$
 272 (covariates) . For the later model, the AIC was used to select the best combination of predictor
 273 variables:

$$AIC = 2\log(PL) + k(edf)$$

274 where PL is the maximised Palm likelihood of the fitted model, and edf the effective degrees
 275 of freedom of the model (Baddeley et al., 2015- section 12.6.4; Tanaka et al., 2008). The AIC
 276 values of the models with different combination of covariates were compared on the 11 areas
 277 for the intensive farms dataset using the standardized difference with null model AIC,

$$\frac{AIC_{null} - AIC_{model_i}}{AIC_{null}}$$

278 where AIC_{null} is the AIC of a LGCP model without covariates and AIC_{model_i} is the AIC of i^{th}
 280 LGCP models with a set of variables. The model showing the greatest (positive) difference
 281 with the AIC_{null} model was selected for both non-stationary models, the iCSR and the iLGCP.
 282 This was implemented with the functions $ppm()$ and $kppm()$ from the R package *spatstat* when
 283 the model was the CSR and LGCP, respectively. The relative importance of each predictor
 284 variable was estimated as the exponential of the coefficient value of a covariate multiplied by
 285 the range of values of the covariate (Baddeley et al., 2015).

287

288

289 We aimed to evaluate the goodness-of-fit of our simulated patterns in their capacity to
290 reproduce both the level of clustering and the location of clusters in comparison to the observed
291 patterns. For each sample area and type of model, and using the best-fit parameters, we
292 simulated 1500 and 8000 point patterns for extensive and intensive datasets, respectively. The
293 number of simulations was chosen to balance the stability of the p-value and computing time
294 (SM – Figure S 4). We implemented the global rank envelope test again to quantify the
295 similarities in the level of clustering. This function allows a point pattern to be characterised
296 independently from the density of points, which enabled the comparison of the p-values across
297 simulations and areas. We then looked at the proportion of sample areas with significant p-
298 values. To evaluate the goodness-of-fit of the simulated patterns in terms of location of the
299 clusters, each sample area was further divided into 64 square quadrats. The correlation
300 coefficient between the observed and modelled number of farms per quadrat for each
301 simulation was computed. Quadrats intersecting the Thai border were removed when less than
302 95% of their area was in Thailand. Quadrat size was chosen to have a sufficient number of
303 quadrats and of points per quadrat to produce a meaningful correlation coefficient (SM - Figure
304 S 5). In addition to goodness-of-fit methods estimated for each model type (CSR, iCSR LGCP
305 and iLGCP) on the calibration area, we also estimated goodness-of-fit methods (global rank
306 envelope test and correlation coefficient) on a different sample area from the model calibration
307 area, henceforth referred to as the validation area.

308

309 **3. Results**

310 Intensive farms were clustered, as assessed by the L-functions (Fig. 3). Extensive farms were
311 randomly distributed, L-function being around the CSR case L-function. Empirical non-
312 stationary L-functions (L-inhom on Fig. 3) were closer to CSR case than the stationary L-
313 functions (L-hom on Fig. 3). All four spatial predictors and their quadratic terms were included
314 in the non-stationary models (iCSR and iLGCP), following the comparison of AIC on the
315 intensive farms dataset (Fig. 4). This intensity function was defined as

316
 317
 318
 319
 320
 321

$$\lambda(u) = \exp(\beta_0 + \beta_1 Hpop(u) + \beta_2 Remot(u) + \beta_3 Crop(u) + \beta_4 Tree(u) + \beta_5 Hpop^2(u) + Remot^2(u) + \beta_7 Crop^2(u) + \beta_8 Tree^2(u))$$

with $\beta_0, \beta_1, \dots, \beta_8$ to parameters to be estimates, *Hpop* the human population density, *Remote* the remoteness, *Crop* the cropland and *Tree* the tree cover.

(a) Intensive dataset

(b) Extensive dataset

CALIBRATION					TRAINING				
Significance threshold	0,001	0,01	0,05	0,1	Significance threshold	0,001	0,01	0,05	0,1
CSR	100	100	100	100	CSR	100	100	100	100
iCSR	91	100	100	100	iCSR	100	100	100	100
LGCP	0	27	64	73	LGCP	0	16	34	45
iLGCP	27	36	73	82	iLGCP	24	53	68	76

VALIDATION					VALIDATION				
Significance threshold	0,001	0,01	0,05	0,1	Significance threshold	0,001	0,01	0,05	0,1
CSR	100	100	100	100	CSR	100	100	100	100
iCSR	82	91	91	100	iCSR	100	100	100	100
LGCP	0	27	64	73	LGCP	50	68	79	79
iLGCP	45	64	73	73	iLGCP	79	89	92	95

322 **Table. 2. Proportions of sample areas with a significant p-value at different significance thresholds.**

323

324 In terms of indicators of level of clustering (Table. 2a and b), measured with the global rank
 325 envelope test, LGCP and iLGCP reproduced the observed level of clustering better than the
 326 random models (CSR and iCSR), having higher p-values in almost all sample areas from both
 327 datasets. CSR and iCSR models were almost always highly significant ($p < 0.05$), thus neither
 328 models explained the observed point patterns. LGCP was more often the best model but did
 329 not explain the data in all sample areas since their p-values were significant in some areas. In
 330 sample areas where a model was not rejected, both LGCP and iLGCP performed well for the
 331 intensive dataset. LGCP and iLGCP were significant at 0.05 in 64% and 73% of cases for the
 332 calibration and the validation. However, LGCP performed better than iLGCP in extensive
 333 dataset. LGCP and iLGCP were significant at the $p < 0.05$ level on extensive dataset, in 34%
 334 and 68% of cases for calibration and 79% and 92% of cases validation. However, the variance

335 of LGCP models was higher than iLGCP models. iLGCP models were then more easily
336 rejected by the global rank envelope as seen with the width of the envelopes (Fig. 5).

337

338 In terms of location of clusters (Fig. 6a and b), the models with covariates (iCSR and iLGCP)
339 performed better than the models without (CSR and LGCP). The two sets of metrics of the
340 iCSR and iLGCP models in the calibration and validation areas had significantly higher
341 correlation coefficients than the other models (CSR and LGCP), for both intensive and
342 extensive farm point patterns. This result was expected since these models are
343 inhomogeneous, having an intensity explained by covariates. The medians of the correlation
344 coefficients of iCSR and iLGCP were generally higher for the extensive than for the intensive
345 dataset. However, correlation coefficients were slightly higher for iCSR models compared to
346 iLGCP models in both calibration and validation area. The medians of the correlation
347 coefficients of the different models (CSR, iCSR, LGCP and iLGCP (calibration and validation))
348 were 0.008, 0.565, 0.004, 0.411, -0.006, 0.521, -0.002 and 0.356 for the intensive dataset and
349 0.006, 0.752, 0.003, 0.631, 0.000, 0.711, 0.007 and 0.576 for the extensive dataset. Taking
350 into account both indices, of the level of clustering and the location of clusters, iLGCP
351 performed the best. We provided as an illustration a simulation produced by the four model
352 types (CSR, iCSR, LGCP and iLGCP) applied to a sample are from intensive and extensive
353 farms datasets and a plot of the observed farm patterns (Fig. 5), along with the plot of the
354 global rank envelope test.

355

356 The coefficients of the different iLGCP model parameters for both intensive and extensive
357 datasets are presented in Fig. 8. Human population density was by far the most important
358 predictor of intensive and extensive models on average, followed by tree cover, cropland and
359 remoteness (Fig. 7), and the relative importance of predictor variables were similar for the
360 intensive and extensive farms.

361

362 **4. Discussion**

363 In this paper, we explored the potential of point pattern simulation models to reproduce real-
364 world distribution of intensive and extensive chicken farms. The implementation of these
365 models allowed to produce a set of discrete and realistic point locations. Our iLGCP models
366 were able to reproduce the level of clustering and the local density of farms better than the
367 other models. LGCP models reproduced the level of clustering, but not the cluster location
368 well, whereas iCSR located the clusters well, but did not capture the level of clustering.
369 Extensive farm distribution was closer to a random distribution than intensive farms, and these
370 simulations benefitted less from using a LGCP. Conversely, intensive farms were more
371 clustered, so the LGCP models reproduced these patterns much better than the random
372 model, but the quality of the prediction of local densities was lower.

373

374 Our result indicated clearly the need to account for clustering in the distribution of intensive
375 farms. Such clustering of farms may enable farmers to benefit from economies of scale (Van
376 Boeckel et al., 2012), or facilitate operations for contract farming. Many farmers in Thailand
377 operate as contractors for large consolidator companies such as Charoen Pokphand (CP).
378 Farms directly owned by CP may also be clustered. Also, as described by (Feder et al., 1985),
379 the adoption of agricultural innovations in developing countries is affected by group influences
380 on individual behaviour. The presence of a well-established, successful, intensive poultry farm
381 may stimulate similar economic activity nearby. The improved prediction of intensive farm
382 locations by including clustering thus makes sense.

383

384 More surprising was the dominance of human population density as a predictor of intensive
385 farms since broiler production in Thailand was previously described as being mainly located
386 around hatcheries, feed mills and processing plants (Costales, 2004; NaRanong, 2007), but
387 these may themselves correlate to human population. The association with human population
388 density could relate to market access, and the model typically placed intensive farms in areas
389 with intermediate human population density, such as in peri-urban areas. The establishment
390 of a chicken farm is thus constrained by a trade-off between market access and the cost of

391 land, which may become prohibitive in more urbanized areas. Our results contrasted with the
392 results of Van Boeckel et al. (2012), who showed cropping factor had a stronger effect than
393 human population in their logistic regression models of presence/absence of intensively raised
394 chickens. This variable was not included in our model since it was not available globally.
395 Methodological differences may also explain the lower effect of some factors. Van Boeckel et
396 al. (2012) analysed the entire extent of Thailand, whereas our models were trained within much
397 smaller spatial units. Further predictors may be worth including, if available at the global level.
398 Other accessibility predictors, such as travel distance to ports where feed could be imported,
399 or where outputs could be exported may improve our predictions. Another global predictor
400 which could provide valuable information on access to service and markets is the location of
401 settlement.

402

403 At the local scale, a degree of “random noise” in the location of intensive farms is inevitable,
404 which we did not expect to capture. The initial establishment of an intensive farm may be
405 influenced both by fine-scale spatial factors (i.e. land availability, location suitability and access
406 to inputs and markets) and by individual farmer characteristics (i.e. where they live, the
407 locations of their other investments, their family history and land ownership). Such factors
408 would be difficult to account for in models at the scale considered here. At the scale of the
409 variables used in our models, several sites may then seem equally suitable for setting up a
410 farm, for example, by having an easy access to markets and inputs such as feed. This does
411 not interfere with our objective to depict a realistic distribution of farms.

412

413 The distribution of extensive farms was less clustered, and more readily predicted by human
414 population density. This fitted our expectations because extensively raised chickens are
415 typically owned as backyard poultry by rural populations (Van Boeckel et al., 2012).

416

417 The resolution of the sample areas should not influence our results, since sample areas were
418 chosen to optimise the variability of situations encountered within Thailand in terms of predictor

419 values and density of farms. The reason why the variability of model performed in the different
420 sample areas could be due to the range of predictor value which differ from one area to
421 another. An analysis on whole Thailand would only deal with its geometry and the number of
422 points in the extensive dataset (leading to computation problems).

423
424 Our results indicate that a producing point-based distribution maps of intensive and extensive
425 flocks is feasible. To use this approach in data-poor countries with a comparable farming
426 system, an important next step will be to validate the model in a different country, but with
427 similar environmental conditions, such as Vietnam, where detailed census data exist.
428 Eventually, it would be interesting to investigate how the extensive and intensive models could
429 predict the distribution of farms according to different levels of intensification. One could
430 imagine high-income countries where 99% of the production is intensive to be best predicted
431 by the intensive model alone, and, conversely, that the extensive model could be tested in low-
432 income countries. In intermediate situations, one could apply both models according to the
433 proportion of extensively raised poultry predicted at the national level by Gilbert et al. (2015).
434 To predict farm locations into these different situations, LGCP models would be applied with
435 the same parameters in neighboring countries or in countries with similar agro-ecologies.
436 Several datasets would thus be required to predict farm distribution into countries from different
437 regions or environments. Further extension of this work will lead to the development of entire
438 farm allocation models, where the total number of animals of an administrative unit could be
439 allocated to farms at locations predicted by the LGCP simulation model in such a way to
440 reproduce a given distribution of animals per farm. While artificial-intelligence-based image
441 processing may soon allow to detect most intensified livestock raising infrastructure
442 automatically, it would not detect middle-size commercial poultry farms, which still exists in
443 large numbers in Thailand, and that can look like a normal building. We believe that statistical
444 approaches such as these still hold value for different settings but also for hind- and forecasting
445 of the farming distribution.

446

447 Other types of livestock production may benefit from similar approaches. Pig farming, for
448 example, is also disconnected from the land and could be subject to similar spatial constraints
449 linked to feed availability and market access. In contrast, the distribution of grazing ruminant
450 farms may have very different spatial determinants. The dependence on large areas for
451 grazing may result in a more homogenous spatial distribution (except for feedlot cattle). Land-
452 use predictor variables such as rangeland or pastures may thus become more important
453 factors.

454
455 Middle- and low-income countries are those where this approach bears the greatest value, in
456 relation to the data scarcity some face, and the co-existence, to varying degrees, of extensive
457 and intensive production. While in Brazil livestock data are available at fine scale, in some
458 other large livestock producing countries, such as China and India, livestock data are only
459 available at coarse resolution. These are precisely where the impact of livestock diseases on
460 livelihoods, animal and human health are greatest (Childs et al., 2007) and where good quality
461 data may help with disease prevention. In high-income countries, where intensive production
462 dominates, results like ours offer an interesting substitute to the original data protected by
463 privacy laws.

464

465 **5. Conclusions**

466 We developed farm distribution models using a point pattern modelling method, which allowed
467 the simulation of chicken farm distributions both in terms of spatial clustering and location of
468 clusters. The methods used here no longer predict livestock distribution as a continuous
469 variable but as a discrete variable (i.e. point locations), which is better suited for situations in
470 which animals are raised in very large numbers in single premises. Upon validation in other
471 countries, this may facilitate several applications in epidemiology or environmental science in
472 countries where such detailed data are lacking, or where livestock data are aggregated to
473 protect privacy.

474 **Acknowledgments**

475 The authors would like to thank the “Fonds pour la formation à la Recherche dans l'Industrie
476 et dans l'Agriculture” (FRIA) and the FNRS PDR “Mapping people and livestock” (PDR
477 T.0073.13) who supported this project. We also thank the Department of Livestock
478 Development, Thailand for chicken census data. Christophe A.N. Biscio is supported by The
479 Danish Council for Independent Research | Natural Sciences, grant DFF – 7014-00074
480 “Statistics for point processes in space and beyond”, and by the “Centre for Stochastic
481 Geometry and Advanced Bioimaging”, funded by grant 8721 from the Villum Foundation.

482

483 **References**

- 484 Baddeley, A., Rubak, E., Turner, R., 2015. Spatial Point Patterns: Methodology and
485 Applications with R. Chapman and Hall/CRC Press,.
- 486 Baddeley, A.J., Møller, J., Waagepetersen, R., 2000. Non- and semi-parametric estimation of
487 interaction in inhomogeneous point patterns. *Statistica Neerlandica* 54, 329–350.
488 <https://doi.org/10.1111/1467-9574.00144>
- 489 Bruhn, M., Munoz, B., Cajka, J., Smith, G., Curry, R., Wagener, D., Wheaton, W., 2012.
490 Synthesized Population Databases: A Geospatial Database of US Poultry Farms. RTI
491 Press, Research Triangle Park, NC.
- 492 Burdett, C.L., Kraus, B.R., Garza, S.J., Miller, R.S., Bjork, K.E., 2015. Simulating the
493 Distribution of Individual Livestock Farms and Their Populations in the United States:
494 An Example Using Domestic Swine (*Sus scrofa domesticus*) Farms. *PLOS ONE* 10,
495 e0140338. <https://doi.org/10.1371/journal.pone.0140338>
- 496 Childs, J.E., Richt, J.A., Mackenzie, J.S., 2007. Introduction: conceptualizing and partitioning
497 the emergence process of zoonotic viruses from wildlife to humans. *Curr. Top.*
498 *Microbiol. Immunol.* 315, 1–31.
- 499 Costales, A., 2004. A review of the Thailand poultry sector. Livestock Sector Report -
500 Thailand elaborated for the FAO-AGAL.
- 501 Delgado, C.L., 1999. Livestock to 2020: the next food revolution. International Food Policy
502 Research Institute ; Food and Agriculture Organization of the United Nations ;
503 International Livestock Research Institute, Washington, D.C.; Rome, Italy; Nairobi,
504 Kenya.
- 505 Emelyanova, I.V., Donald, G.E., Miron, D.J., Henry, D.A., Garner, M.G., 2009. Probabilistic
506 Modelling of Cattle Farm Distribution in Australia. *Environmental Modeling &*
507 *Assessment* 14, 449–465. <https://doi.org/10.1007/s10666-008-9140-z>
- 508 Feder, G., Just, R., Zilberman, D., 1985. Adoption of Agricultural Innovations in Developing
509 Countries: A Survey. *Economic Development and Cultural Change* 33, 255–98.
- 510 Fritz, S., See, L., McCallum, I., You, L., Bun, A., Moltchanova, E., Duerauer, M., Albrecht, F.,
511 Schill, C., Perger, C., Havlik, P., Mosnier, A., Thornton, P., Wood-Sichra, U., Herrero,
512 M., Becker-Reshef, I., Justice, C., Hansen, M., Gong, P., Abdel Aziz, S., Cipriani, A.,
513 Cumani, R., Cecchi, G., Conchedda, G., Ferreira, S., Gomez, A., Haffani, M.,
514 Kayitakire, F., Malanding, J., Mueller, R., Newby, T., Nonguierma, A., Olusegun, A.,
515 Ortner, S., Rajak, D.R., Rocha, J., Schepaschenko, D., Schepaschenko, M.,
516 Terekhov, A., Tiangwa, A., Vancutsem, C., Vintrou, E., Wenbin, W., van der Velde,

517 M., Dunwoody, A., Kraxner, F., Obersteiner, M., 2015. Mapping global cropland and
518 field size. *Global Change Biology* 21, 1980–1992. <https://doi.org/10.1111/gcb.12838>

519 Gerber, P.J., Steinfeld, H., Henderson, B., Mottet, A., Opio, C., Dijkman, J., Falcucci, A.,
520 Tempio, G., 2013. Tackling climate change through livestock: a global assessment of
521 emissions and mitigation opportunities. xxi + 115 pp.

522 Gilbert, M., Conchedda, G., Van Boeckel, T.P., Cinardi, G., Linard, C., Nicolas, G.,
523 Thanapongtharm, W., D'Aiotti, L., Wint, W., Newman, S.H., Robinson, T.P., 2015.
524 Income Disparities and the Global Distribution of Intensively Farmed Chicken and
525 Pigs. *PLOS ONE* 10, e0133381. <https://doi.org/10.1371/journal.pone.0133381>

526 Gilbert, M., Nicolas, G., Cinardi, G., Van Boeckel, T., Vanwambeke, S., Wint, G., In press.
527 Global distribution data for cattle, buffaloes, horses, sheep, goats, pigs, chickens and
528 ducks in 2010. *Nature Scientific Data*.

529 Hansen, M.C., Potapov, P.V., Moore, R., Hancher, M., Turubanova, S.A., Tyukavina, A.,
530 Thau, D., Stehman, S.V., Goetz, S.J., Loveland, T.R., Kommareddy, A., Egorov, A.,
531 Chini, L., Justice, C.O., Townshend, J.R.G., 2013. High-Resolution Global Maps of
532 21st-Century Forest Cover Change. *Science* 342, 850–853.
533 <https://doi.org/10.1126/science.1244693>

534 Jones, B.A., Grace, D., Kock, R., Alonso, S., Rushton, J., Said, M.Y., McKeever, D., Mutua,
535 F., Young, J., McDermott, J., Pfeiffer, D.U., 2013a. Zoonosis emergence linked to
536 agricultural intensification and environmental change. *Proceedings of the National
537 Academy of Sciences* 110, 8399–8404. <https://doi.org/10.1073/pnas.1208059110>

538 Jones, B.A., Grace, D., Kock, R., Alonso, S., Rushton, J., Said, M.Y., McKeever, D., Mutua,
539 F., Young, J., McDermott, J., Pfeiffer, D.U., 2013b. Zoonosis emergence linked to
540 agricultural intensification and environmental change. *Proceedings of the National
541 Academy of Sciences* 110, 8399–8404. <https://doi.org/10.1073/pnas.1208059110>

542 Leibler, J.H., Otte, J., Roland-Holst, D., Pfeiffer, D.U., Soares Magalhaes, R., Rushton, J.,
543 Graham, J.P., Silbergeld, E.K., 2009. Industrial Food Animal Production and Global
544 Health Risks: Exploring the Ecosystems and Economics of Avian Influenza.
545 *EcoHealth* 6, 58–70. <https://doi.org/10.1007/s10393-009-0226-0>

546 Li, K.S., Guan, Y., Wang, J., Smith, G.J.D., Xu, K.M., Duan, L., Rahardjo, A.P.,
547 Puthavathana, P., Buranathai, C., Nguyen, T.D., Estoepongastie, A.T.S., Chaisingh,
548 A., Auewarakul, P., Long, H.T., Hanh, N.T.H., Webby, R.J., Poon, L.L.M., Chen, H.,
549 Shortridge, K.F., Yuen, K.Y., Webster, R.G., Peiris, J.S.M., 2004. Genesis of a highly
550 pathogenic and potentially pandemic H5N1 influenza virus in eastern Asia. *Nature*
551 430, 209–213. <https://doi.org/10.1038/nature02746>

552 Martin, M.K., Helm, J., Patyk, K.A., 2015. An approach for de-identification of point locations
553 of livestock premises for further use in disease spread modeling. *Preventive
554 Veterinary Medicine* 120, 131–140. <https://doi.org/10.1016/j.prevetmed.2015.04.010>

555 Mennerat, A., Nilsen, F., Ebert, D., Skorpung, A., 2010. Intensive Farming: Evolutionary
556 Implications for Parasites and Pathogens. *Evolutionary Biology* 37, 59–67.
557 <https://doi.org/10.1007/s11692-010-9089-0>

558 Møller, J., Syversveen, A.R., Waagepetersen, R.P., 1998. Log Gaussian Cox Processes.
559 *Scandinavian Journal of Statistics* 25, 451–482. <https://doi.org/10.1111/1467-9469.00115>

560

561 Monne, I., Fusaro, A., Nelson, M.I., Bonfanti, L., Mulatti, P., Hughes, J., Murcia, P.R., Schivo,
562 A., Valastro, V., Moreno, A., Holmes, E.C., Cattoli, G., 2014. Emergence of a Highly
563 Pathogenic Avian Influenza Virus from a Low-Pathogenic Progenitor. *Journal of
564 Virology* 88, 4375–4388. <https://doi.org/10.1128/JVI.03181-13>

565 Mrkvička, T., Hahn, U., Myllymäki, M., 2016. A one-way ANOVA test for functional data with
566 graphical interpretation. *arXiv:1612.03608 [stat]*.

567 Mrkvička, T., Myllymäki, M., Hahn, U., 2017. Multiple Monte Carlo testing, with applications in
568 spatial point processes. *Stat Comput* 27, 1239–1255. <https://doi.org/10.1007/s11222-016-9683-9>

569

570 Myllymäki, M., Mrkvička, T., Grabarnik, P., Sejjo, H., Hahn, U., 2017. Global envelope tests
571 for spatial processes. *Journal of the Royal Statistical Society: Series B (Statistical*
572 *Methodology)* 79, 381–404. <https://doi.org/10.1111/rssb.12172>

573 NaRanong, V., 2007. Structural changes in Thailand's poultry sector and its social
574 implications. Thailand Development Research Institute, Bangkok, Thailand.

575 Nelson, A., 2008. Travel time to major cities: A global map of Accessibility. Global
576 Environment Monitoring Unit—Joint Research Centre of the European Commission,
577 Ispra, Italy.

578 Neumann, K., Elbersen, B.S., Verburg, P.H., Staritsky, I., Pérez-Soba, M., Vries, W. de,
579 Rienks, W.A., 2009. Modelling the spatial distribution of livestock in Europe.
580 *Landscape Ecol* 24, 1207. <https://doi.org/10.1007/s10980-009-9357-5>

581 Okabe, A., Sugihara, K., Kendall, D.G., Boots, B., 2000. Spatial tessellations: concepts and
582 applications of Voronoi diagrams, 2nd ed. ed, Wiley series in probability and
583 statistics. Wiley, New York.

584 Prosser, D.J., Wu, J., Ellis, E.C., Gale, F., Van Boeckel, T.P., Wint, W., Robinson, T., Xiao,
585 X., Gilbert, M., 2011. Modelling the distribution of chickens, ducks, and geese in
586 China. *Agriculture, Ecosystems & Environment* 141, 381–389.
587 <https://doi.org/10.1016/j.agee.2011.04.002>

588 Pulliam, J.R.C., Epstein, J.H., Dushoff, J., Rahman, S.A., Bunning, M., Jamaluddin, A.A.,
589 Hyatt, A.D., Field, H.E., Dobson, A.P., Daszak, P., the Henipavirus Ecology Research
590 Group (HERG), 2012. Agricultural intensification, priming for persistence and the
591 emergence of Nipah virus: a lethal bat-borne zoonosis. *Journal of The Royal Society*
592 *Interface* 9, 89–101. <https://doi.org/10.1098/rsif.2011.0223>

593 Reeves, A., 2012. Construction and evaluation of epidemiologic simulation models for the
594 within- and among-unit spread and control of infectious diseases of livestock and
595 poultry (Thesis). Colorado State University. Libraries.

596 Robinson, T.P., Wint, G.R.W., Conchedda, G., Van Boeckel, T.P., Ercoli, V., Palamara, E.,
597 Cinardi, G., D'Aiotti, L., Hay, S.I., Gilbert, M., 2014. Mapping the Global Distribution of
598 Livestock. *PLoS ONE* 9, e96084. <https://doi.org/10.1371/journal.pone.0096084>

599 Slingenbergh, J., Cecchi, G., Engering, A., Hogerwerf, L., 2013. World livestock 2013:
600 changing disease landscapes.

601 Smil, V., 2002. Worldwide transformation of diets, burdens of meat production and
602 opportunities for novel food proteins. *Enzyme and Microbial Technology* 30, 305–311.

603 Steinfeld, H., 2004. The livestock revolution—a global veterinary mission. *Veterinary*
604 *Parasitology* 125, 19–41. <https://doi.org/10.1016/j.vetpar.2004.05.003>

605 Steinfeld, H., Gerber, P., Wassenaar, T.D., Castel, V., de Haan, C., 2006. Livestock's long
606 shadow: environmental issues and options. Food & Agriculture Org.

607 Tanaka, U., Ogata, Y., Stoyan, D., 2008. Parameter Estimation and Model Selection for
608 Neyman-Scott Point Processes. *Biometrical Journal* 50, 43–57.
609 <https://doi.org/10.1002/bimj.200610339>

610 Tildesley, M.J., House, T.A., Bruhn, M.C., Curry, R.J., O'Neil, M., Allpress, J.L.E., Smith, G.,
611 Keeling, M.J., 2010. Impact of spatial clustering on disease transmission and optimal
612 control. *Proceedings of the National Academy of Sciences* 107, 1041–1046.
613 <https://doi.org/10.1073/pnas.0909047107>

614 Tildesley, M.J., Ryan, S.J., 2012. Disease Prevention versus Data Privacy: Using Landcover
615 Maps to Inform Spatial Epidemic Models. *PLoS Comput Biol* 8.
616 <https://doi.org/10.1371/journal.pcbi.1002723>

617 Van Boeckel, T.P., Gandra, S., Ashok, A., Caudron, Q., Grenfell, B.T., Levin, S.A.,
618 Laxminarayan, R., 2014. Global antibiotic consumption 2000 to 2010: an analysis of
619 national pharmaceutical sales data. *The Lancet infectious diseases* 14, 742–750.

620 Van Boeckel, T.P., Prosser, D., Franceschini, G., Biradar, C., Wint, W., Robinson, T., Gilbert,
621 M., 2011. Modelling the distribution of domestic ducks in Monsoon Asia. *Agric*
622 *Ecosyst Environ* 141, 373–380. <https://doi.org/10.1016/j.agee.2011.04.013>

623 Van Boeckel, T.P., Thanapongtharm, W., Robinson, T., D'Aiotti, L., Gilbert, M., 2012.
624 Predicting the distribution of intensive poultry farming in Thailand. *Agric Ecosyst*
625 *Environ* 149, 144–153. <https://doi.org/10.1016/j.agee.2011.12.019>
626 Wint, W., Robinson, T., FAO, 2007. *Gridded livestock of the world*. Food and Agriculture
627 Organization of the United Nations, Rome.
628

629 **Figure captions**

630 **Fig. 1. Predictors values.** Human population density (logarithm of human population density
631 in heads per km²), Remoteness (travel time to province capital cities in minute), Cropland
632 (percent of pixel covered by crops) and Tree cover (percent of pixel covered by forest).

633 **Fig. 2. Sample areas defined for the study** (a) 11 sample areas of 200 km length side defined
634 for the intensive dataset (b) 38 sample areas of 112 km length side defined for the extensive
635 dataset.

636 **Fig. 3. Descriptive analysis of intensive and extensive farms datasets using stationary
637 and non-stationary L-functions.** Each dashed line represents the empirical L-function, $L(r)$,
638 estimated from the observed point pattern from each sample area, and r is the radius in meters.
639 Comparing the empirical L-functions of a point pattern with the theoretical L-function of a
640 completely spatial randomness (CSR) enables to determine if a pattern is clustered, random
641 or regular, with L-functions higher than, close to or lower than the CSR case, respectively.
642 Dashed grey line: stationary empirical L-function, $L_{\text{hom}}(r)$, for each sample area; dashed blue
643 lines: non-stationary empirical L-function, $L_{\text{inhom}}(r)$, for each sample area; black line: theoretical
644 L-function, $L_{\text{poisson}}(r)$, of a CSR.

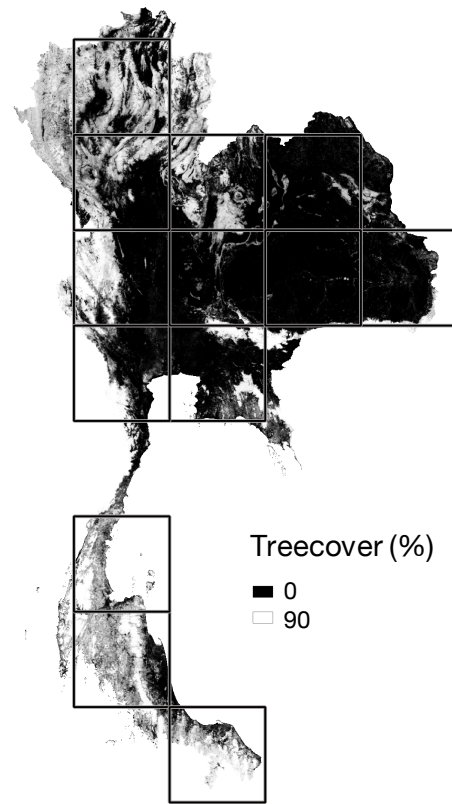
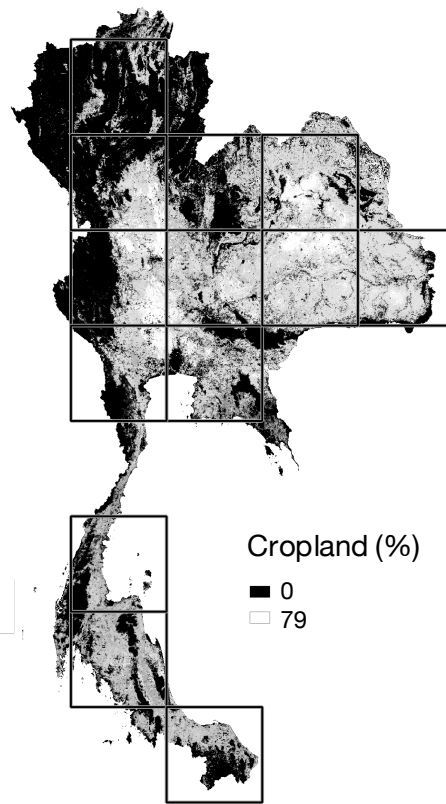
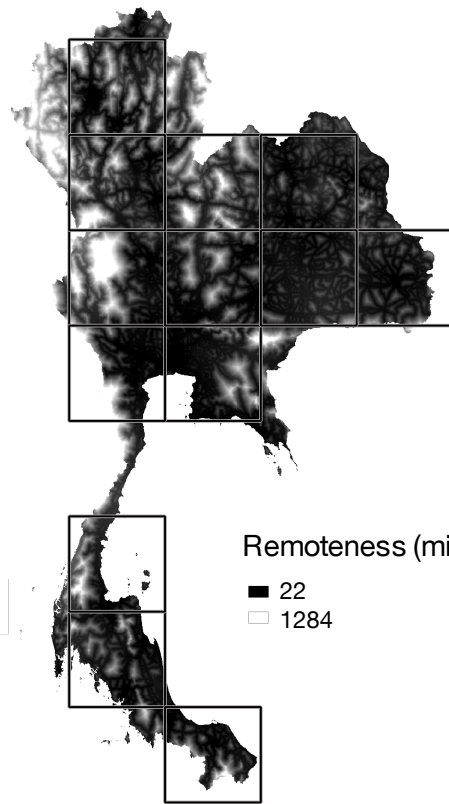
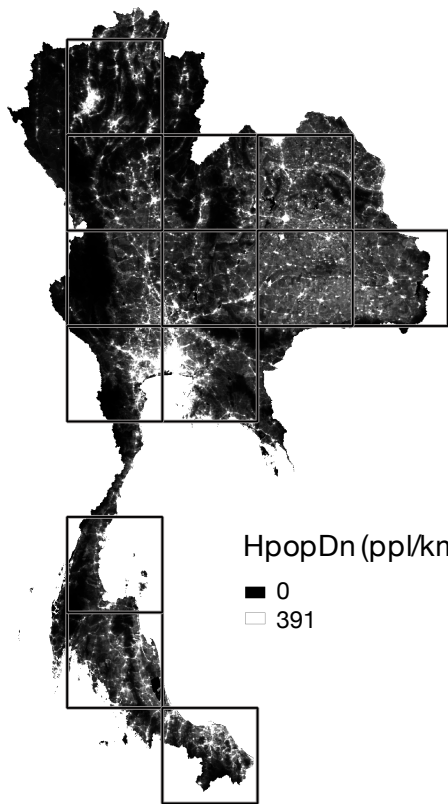
645 **Fig. 4. Comparison of models with different combination of covariates (human
646 population density (Hpop), remoteness (Remot), cropland (Crop) and tree cover (Tree))
647 with AIC standardized difference.** The first model is fitted with Hpop, the second model is
648 fitted with Hpop + Remot, the third model is fitted with Hpop + Remot + Crop, the fourth is fitted
649 with Hpop + Remot + Crop + Tree, for the four variables de square term is also added. Grey
650 lines represent values for each sample area of the intensive dataset and the black line the
651 average line.

652 **Fig. 5. The observed point pattern and examples of simulations produced by the four**
653 **model types along with the global rank envelope test, for a sample area for both**
654 **intensive and extensive datasets.** The four models were the completely spatial randomness
655 (CSR), the CSR with covariates (iCSR), the Log-Gaussian Cox process (LGCP) and the LGCP
656 with covariates (iLGCP). In the global rank envelope test, with extreme rank lengths: dashed
657 lines represent the 95% global envelope with 8,000 and 1,500 simulations for intensive and
658 extensive datasets, respectively; black line: the empirical L-function estimated from the
659 observed point pattern; and red points: the points of the empirical L-function which are outside
660 the envelope.

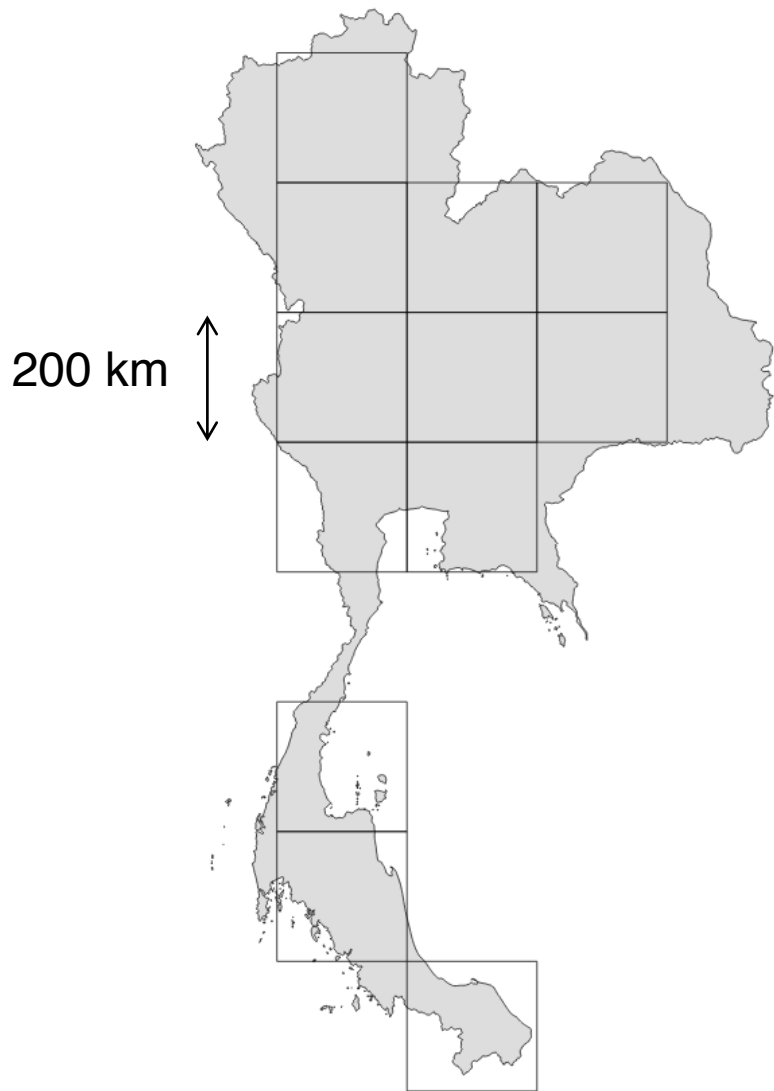
661 **Fig. 6. Correlation coefficient between the numbers of points per quadrat for all**
662 **quadrats in observed and each simulated pattern for a) extensive and b) intensive**
663 **farms.** The distribution of correlation coefficient values for all simulations (1500 and 8000
664 simulations for extensive and intensive datasets, respectively) on each area is plotted for the
665 four models (completely spatial randomness (CSR), the CSR with covariates (iCSR), the Log-
666 Gaussian Cox process (LGCP) and the LGCP with covariates (iLGCP)), for calibration and
667 validations areas.

668 **Fig. 7. Relative covariates importance of iLGCP models by sample area with covariates**
669 **for a) intensive and b) extensive dataset.** Logarithm of the relative importance of each
670 covariate and its quadratic term: human population density (Hpop + Hpop²), tree cover (Tree
671 + Tree²), cropland (Crop + Crop²) and the remoteness or accessibility (Remot + Remot²).

672 **Fig. 8. Boxplots of the coefficients from the different iLGCP model parameters fitted on**
673 **each sample area** (α , σ^2 and $\beta_0, \beta_1 \dots \beta_8$). In LGCP models, the covariance is defined as $C_0(r)$
674 $= \sigma^2 \exp(-r/\alpha)$ where σ^2 is the variance and α the scale parameter and the intensity function
675 was defined as $\lambda(\mathbf{u}) =$
676 $\exp(\beta_0 + \beta_1 Hpop(\mathbf{u}) + \beta_2 Crop(\mathbf{u}) + \beta_3 Tree(\mathbf{u}) + \beta_4 Remot(\mathbf{u}) + \beta_5 Hpop^2(\mathbf{u}) + \beta_6 Crop^2(\mathbf{u}) + \beta_7 Tree^2(\mathbf{u}) + \beta_8 Remot^2(\mathbf{u}))$
677 .
678



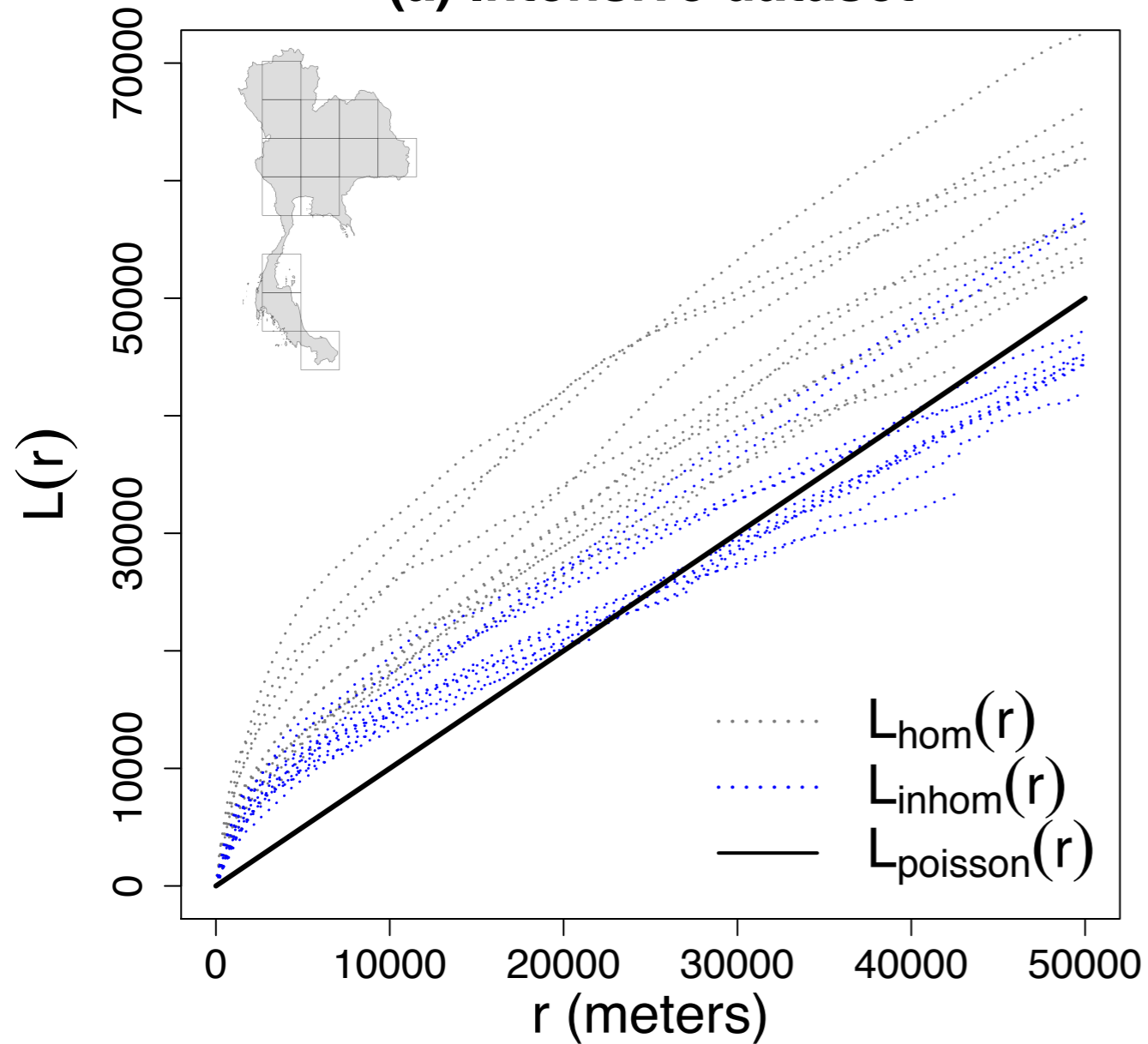
(a) Intensive farms



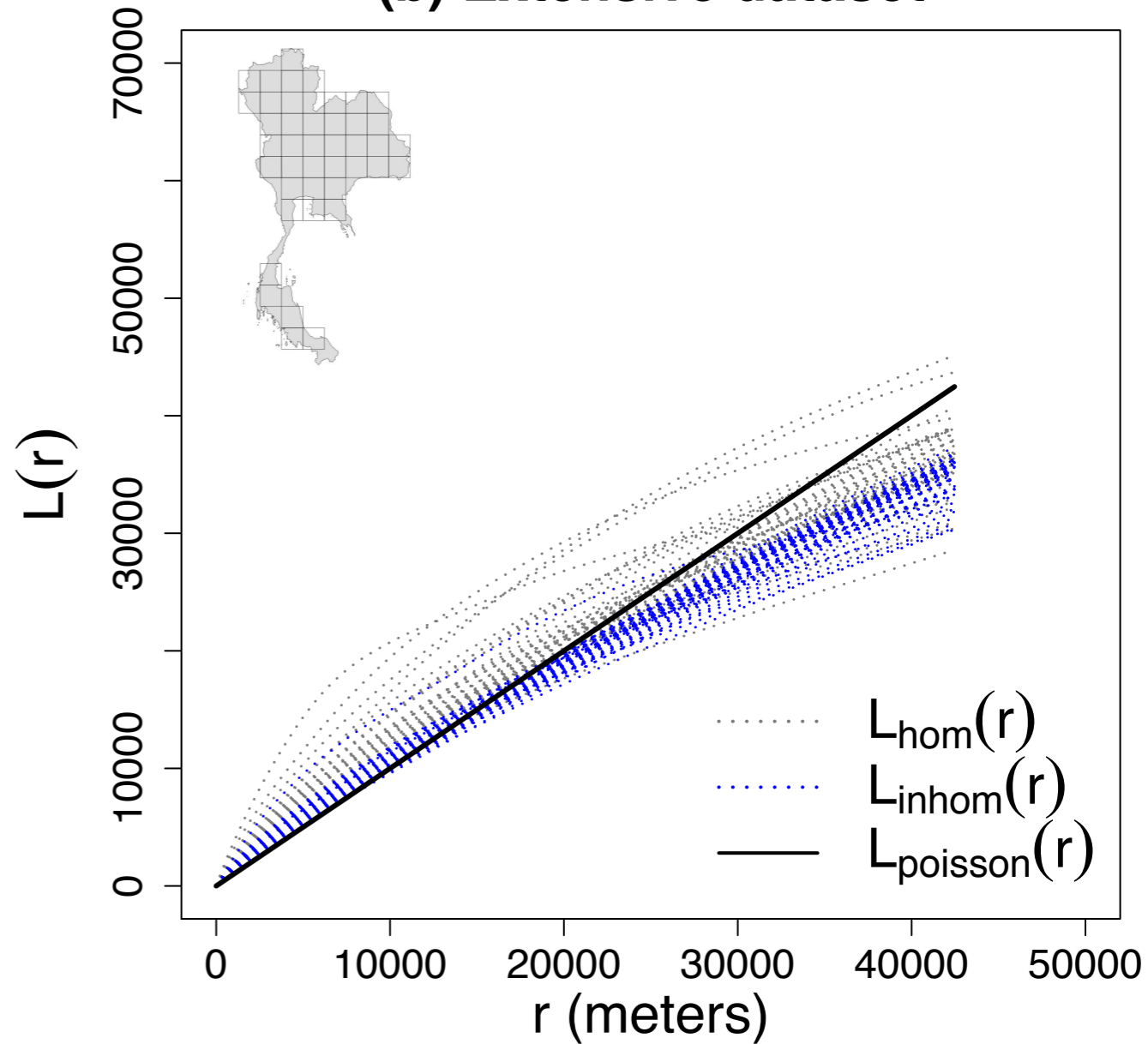
(b) Extensive farms



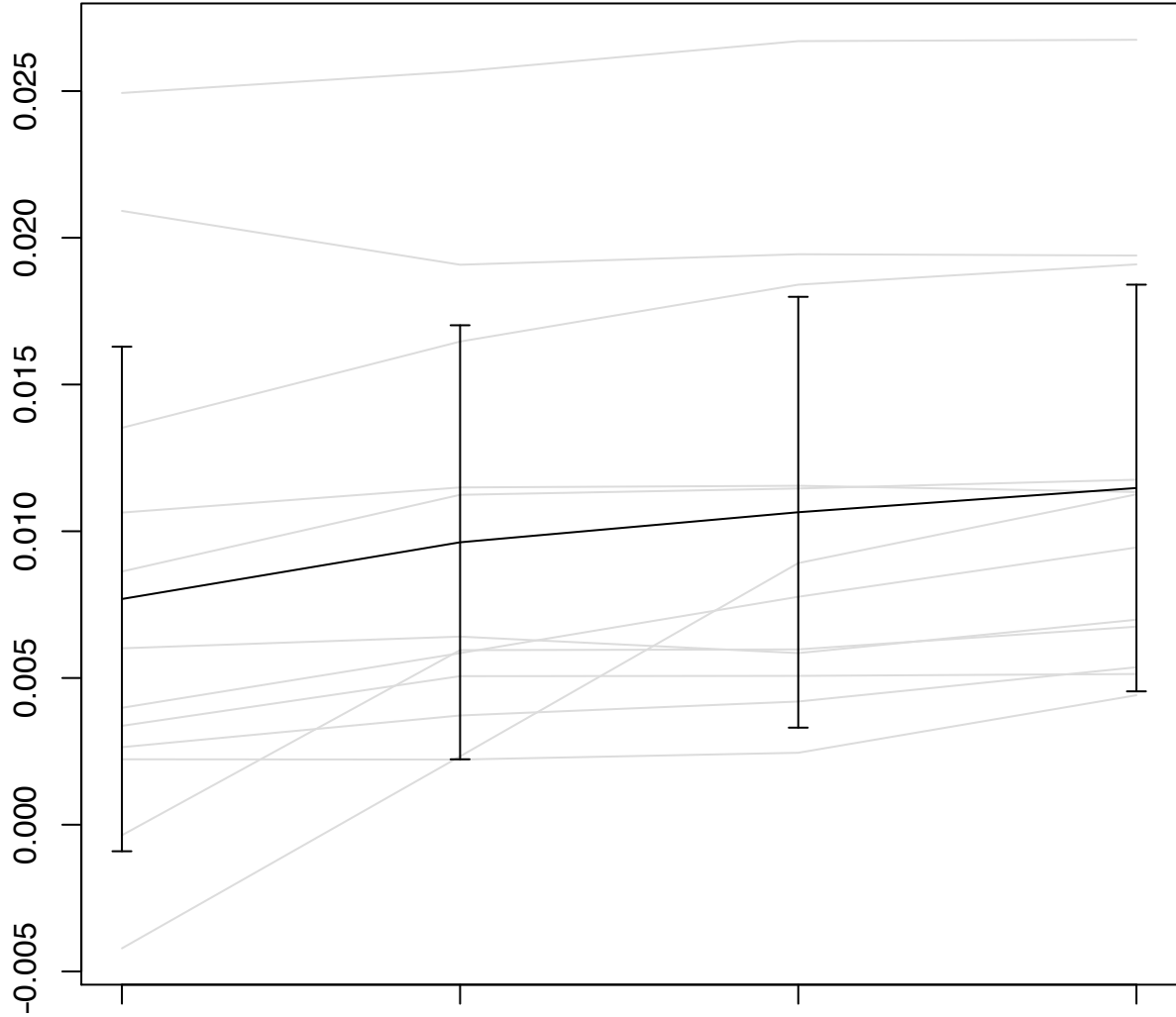
(a) Intensive dataset



(b) Extensive dataset



Standardized AIC difference



Hpop +
Hpop²

Hpop + Remot +
Hpop² + Remot²

Hpop + Remot + Crop +
Hpop² + Remot² + Crop²

Hpop + Remot + Crop + Tree +
Hpop² + Remot² + Crop² + Tree²

(a) Intensive dataset
Calibration area

(b) Extensive dataset
Calibration area

Observed

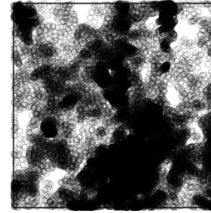
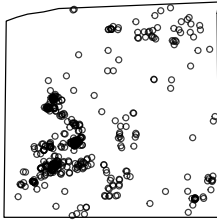


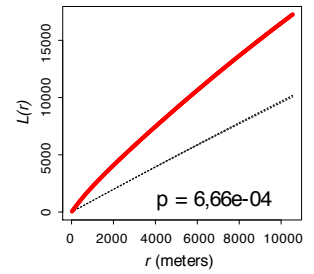
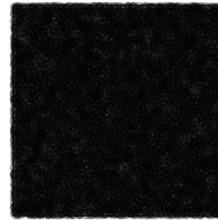
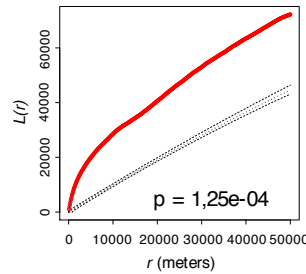
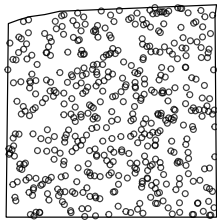
Illustration of a simulation

Global rank envelope test (using extreme rank length)

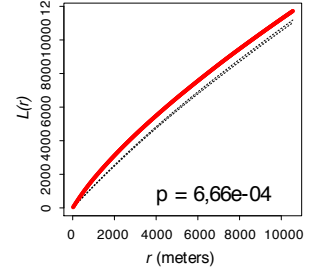
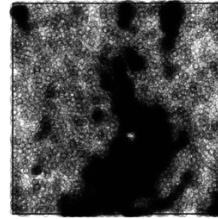
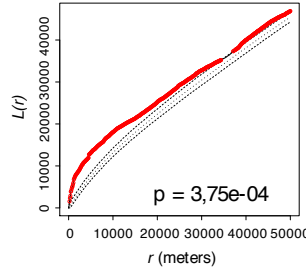
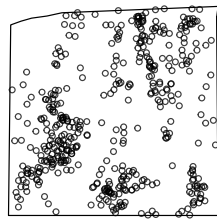
Illustration of a simulation

Global rank envelope test (using extreme rank length)

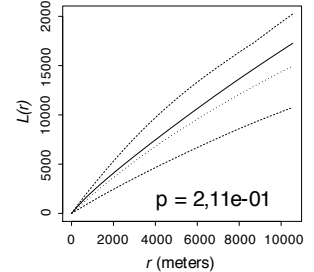
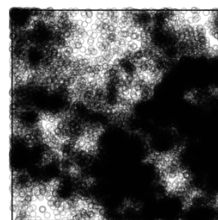
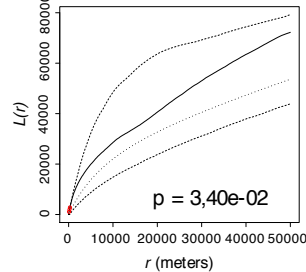
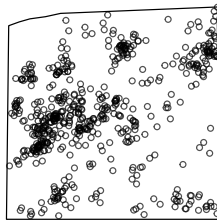
CSR



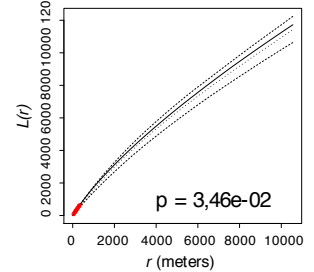
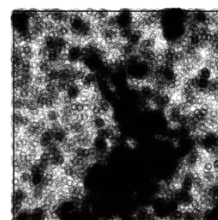
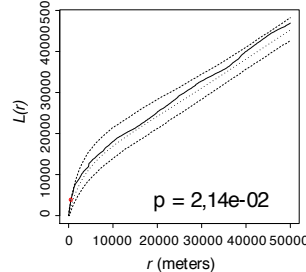
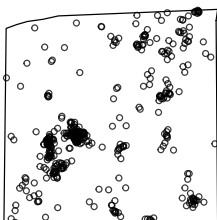
iCSR



LGCP



iLGCP

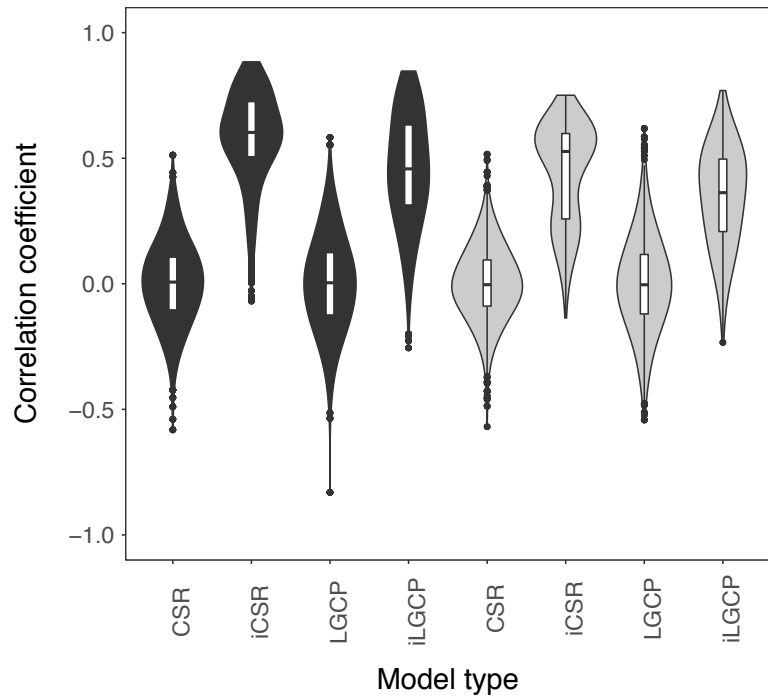


— empirical L-function

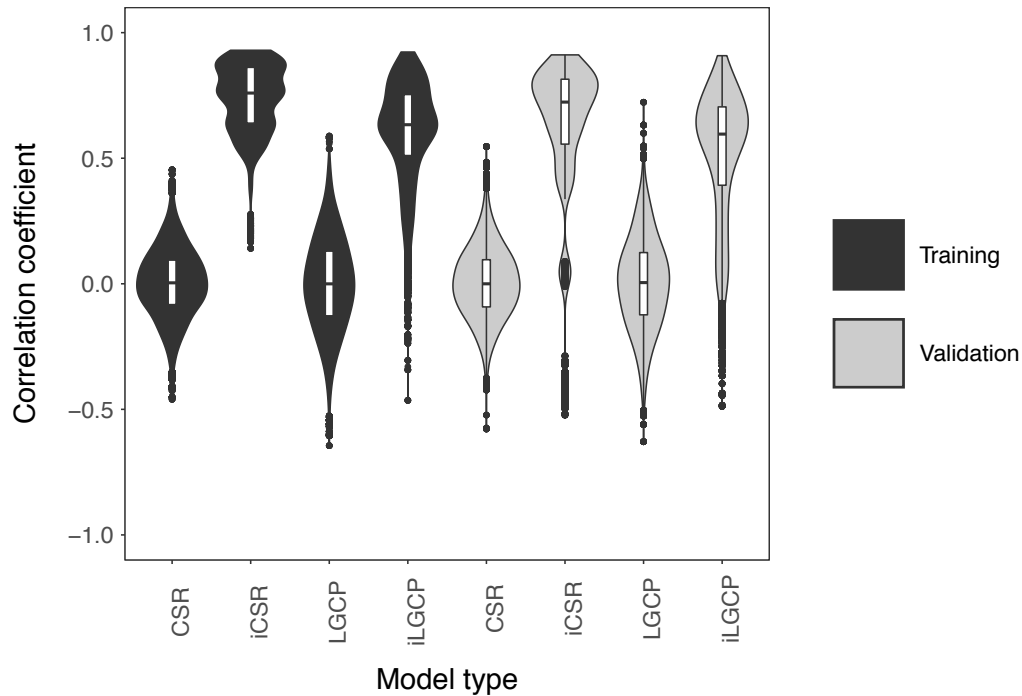
○ point outside the envelope

----- 95% global envelope

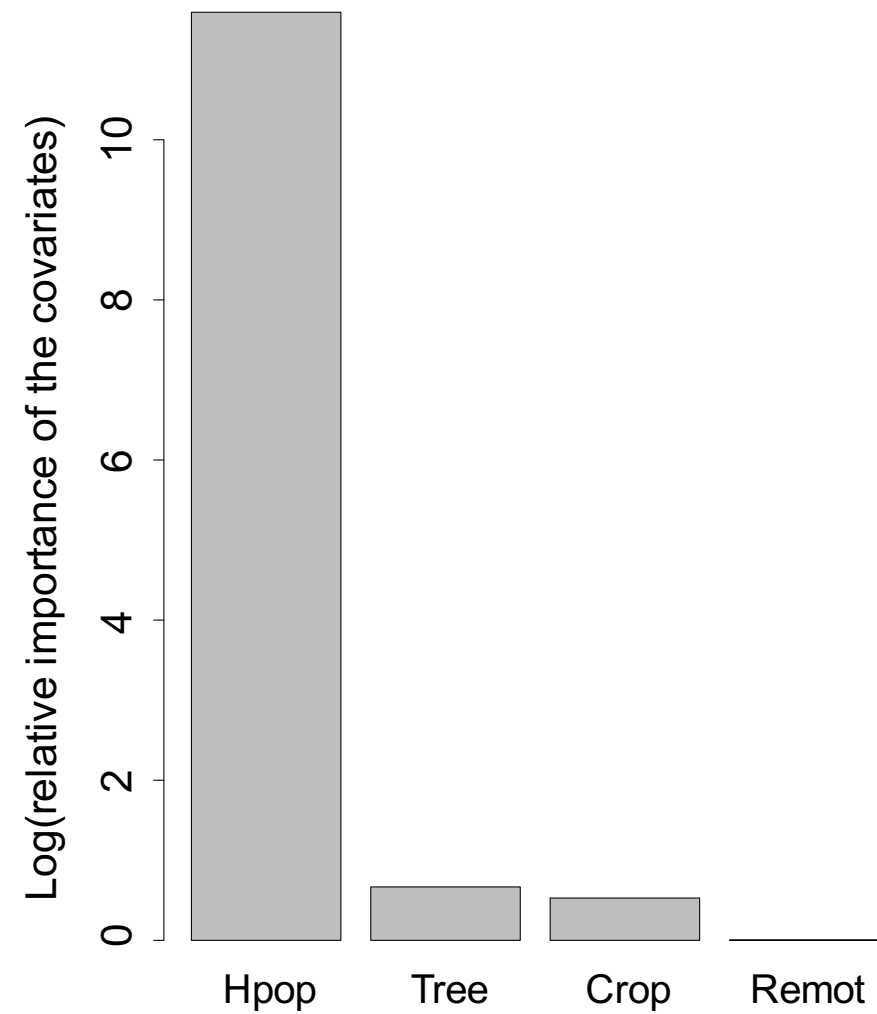
(a) Intensive dataset



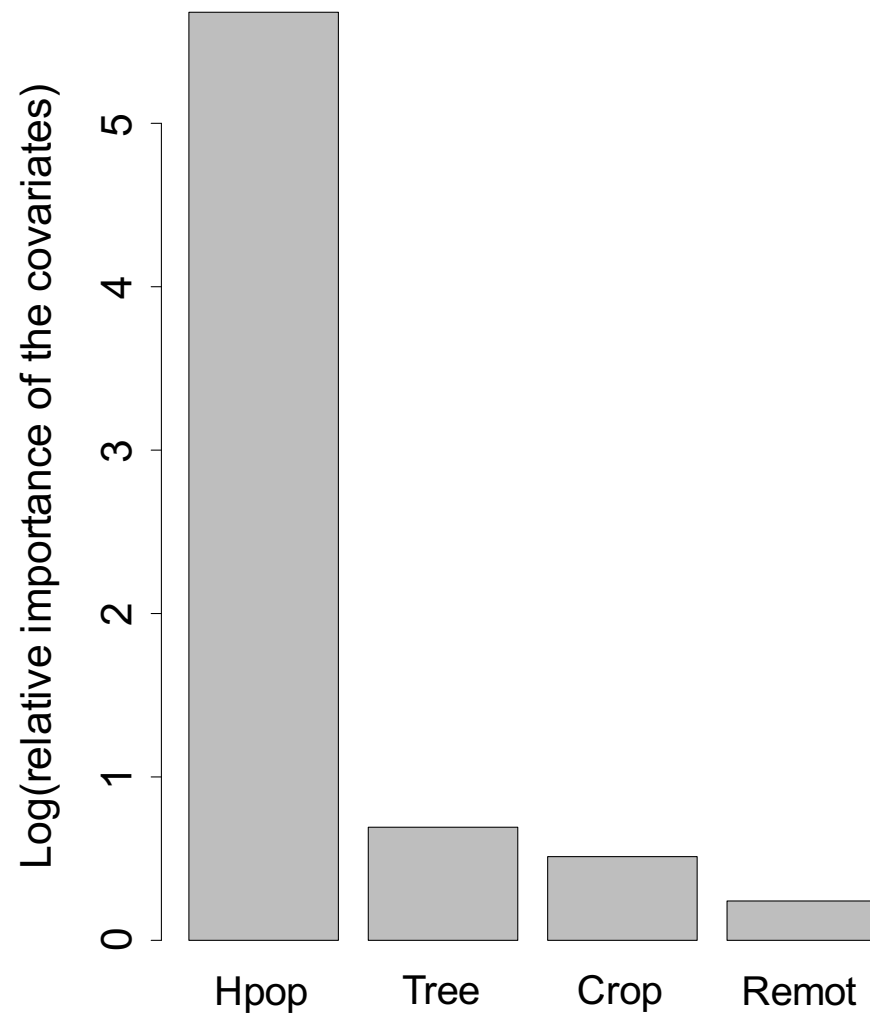
(b) Extensive dataset

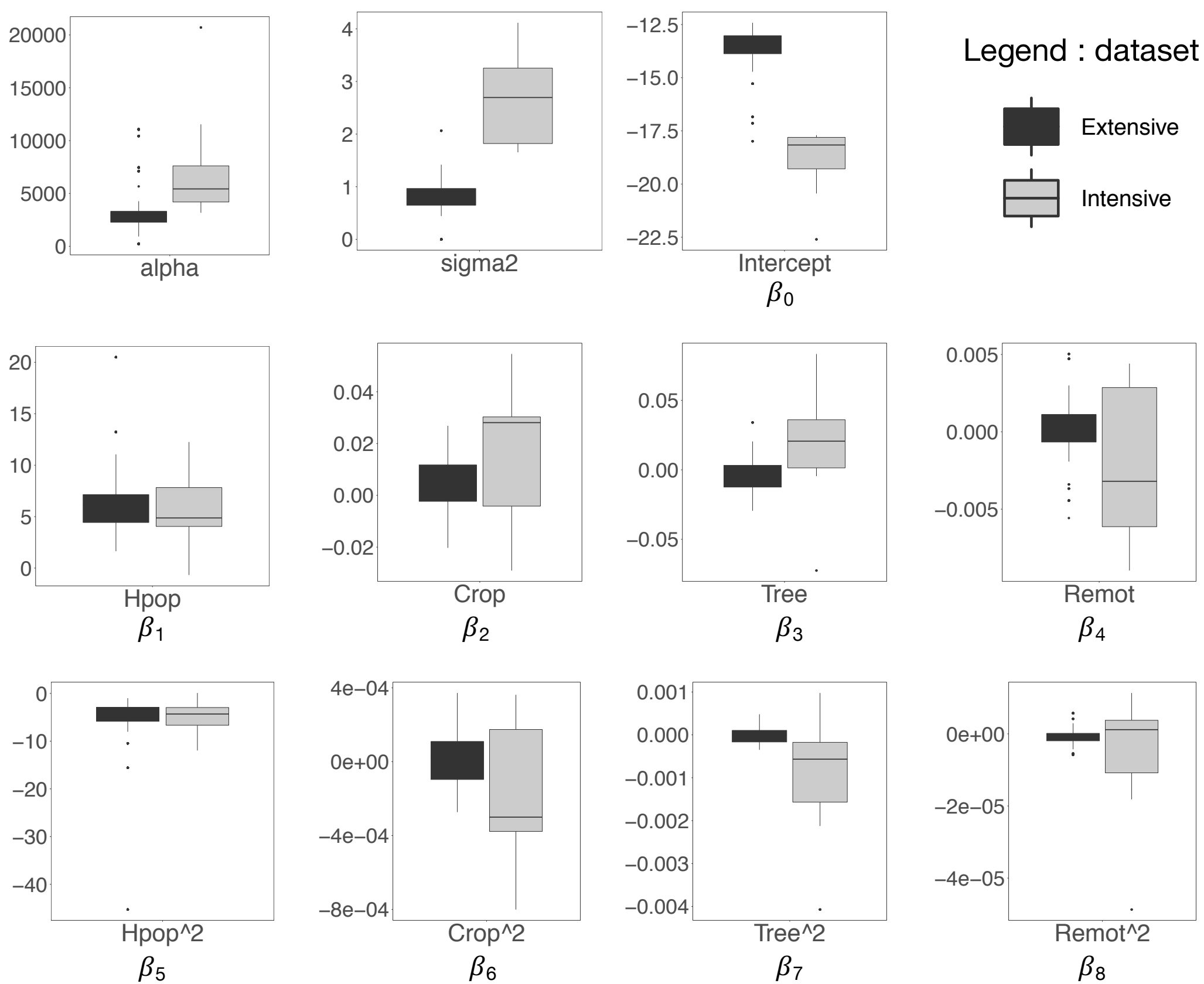


(a) Intensive systems



(b) Extensive systems





Supplementary materials to « Point pattern simulation modelling of extensive and intensive chicken farming in Thailand: accounting for clustering and landscape characteristics »

Celia Chaiban, Christophe Biscio, Weerapong Thanapongtharm, Michael Tildesley, Xiangming Xiao, Timothy P Robinson, Sophie O Vanwambeke, Marius Gilbert

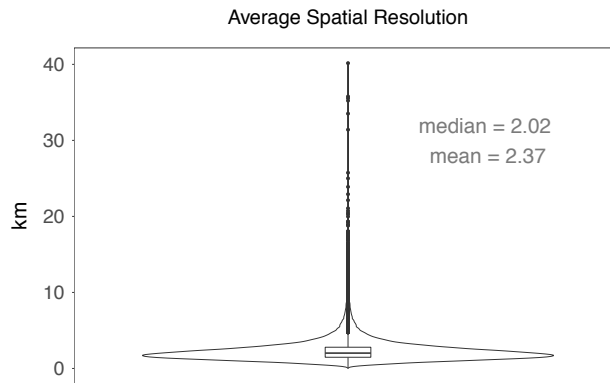
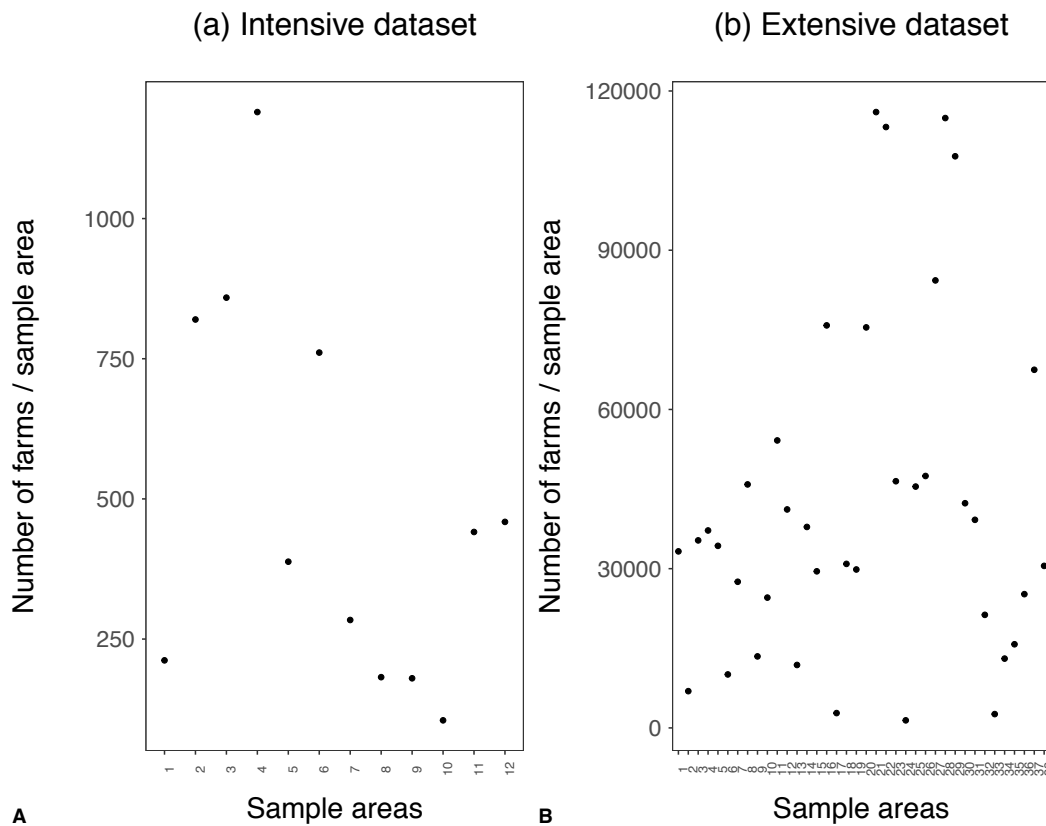


Figure S 1. Violin plot of the distribution of the average spatial resolution (root square of the area) of Voronoi polygons in kilometers



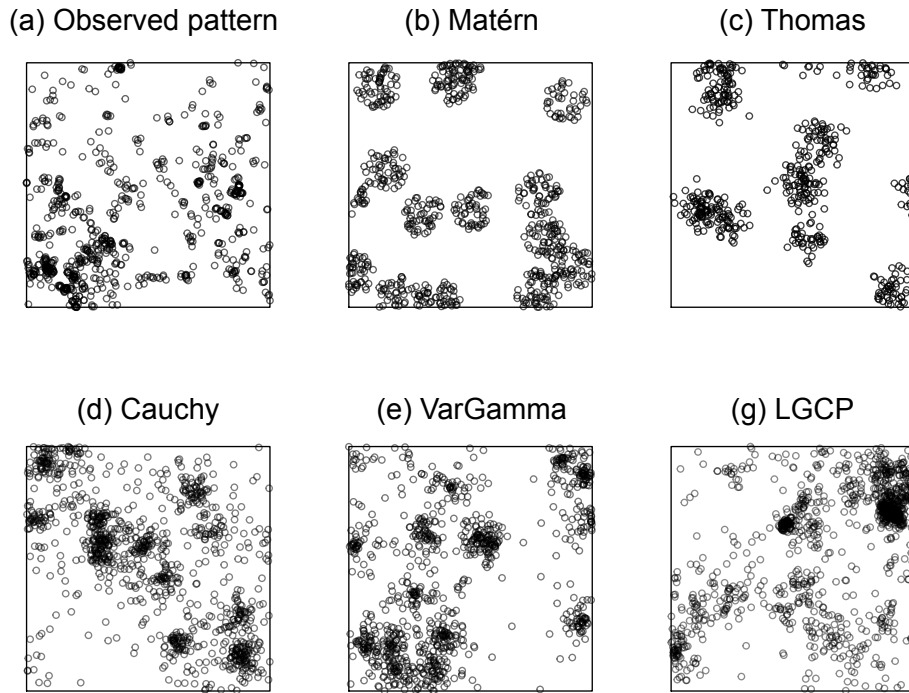


Figure S 2. Observed point pattern of a sample area from Thailand (a) compared to a simulation obtained by the different cox processes. (b) a Matérn process model (c) a Thomas process model (d) a Cauchy process model (e) a Variance Gamma process model (g) a Log-Gaussian Cox Processes model.

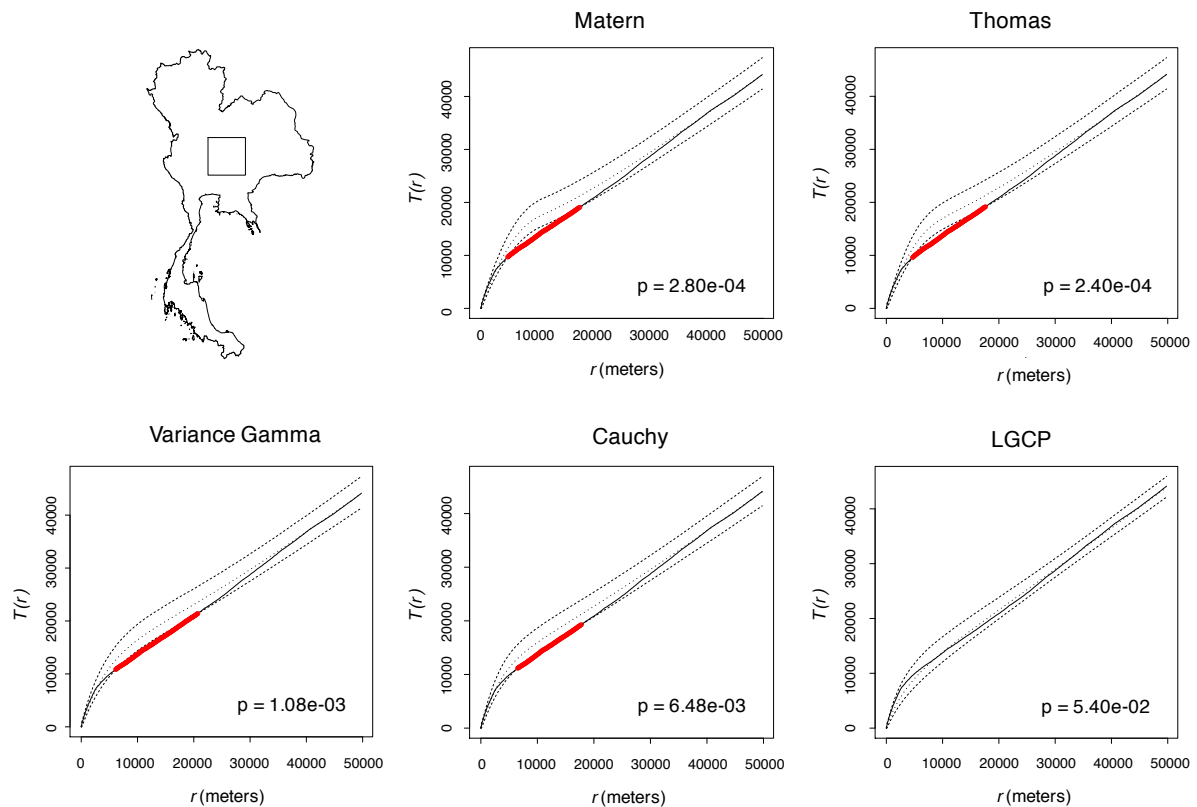


Figure S 3. Global rank envelope test on the five different processes, Matérn, Thomas, Cauchy, Variance Gamma and Log-Gaussian Cox Processes (LGCP), based on the L-function.

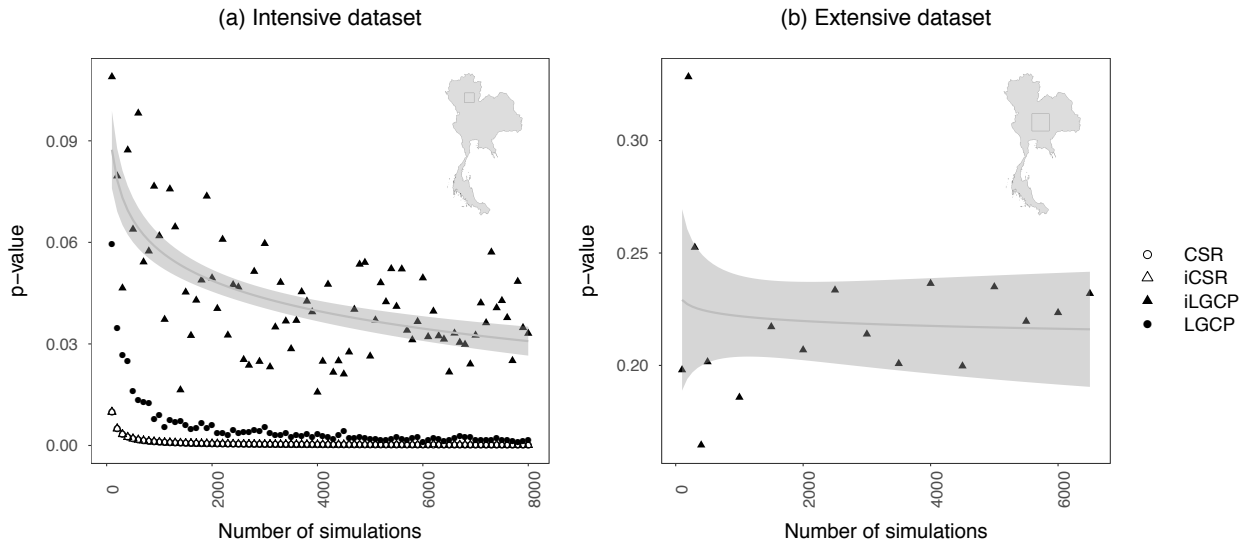


Figure S 4. Extreme rank envelope test p-values with different number of simulations for extensive (a) and intensive (b) datasets, on a sample area of Thailand.

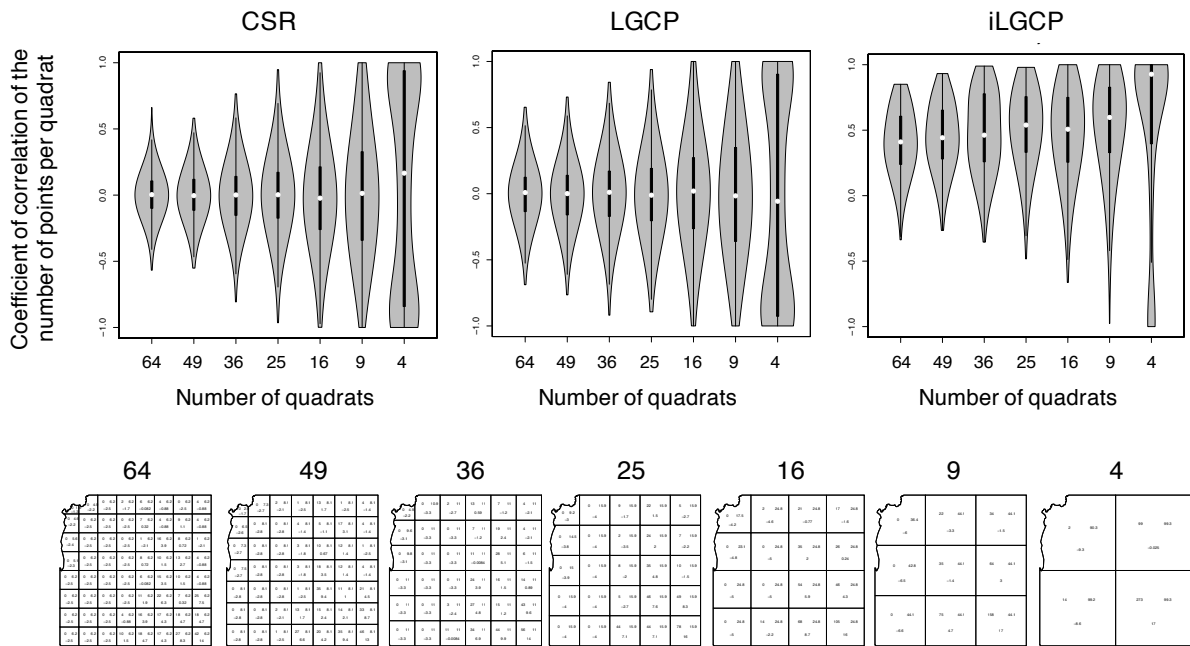


Figure S 5. Coefficient of correlation on the number of points per quadrats for different quadrat sizes for the Complete Spatial Randomness (CSR), the log-Gaussian cox Processes (LGCP) and the LGCP with covariates (iLGCP).

INTENSIVE DATASET

CALIBRATION

	B	D	K	L	N	O
CSR	0,000125 ***	0,000125 ***	0,000125 ***	0,000125 ***	0,000125 ***	0,000125 ***
iCSR	0,000375 ***	0,000125 ***	0,000125 ***	0,000125 ***	0,000250 ***	0,000125 ***
LGCP	0,502937	0,091739 .	0,001125 **	0,026747 *	0,004749 **	0,030746 *
iLGCP	0,533558	0,012373 *	0,000125 ***	0,001250 **	0,000250 ***	0,034746 *

	P	S	t	U	X
CSR	0,000125 ***	0,000125 ***	0,000125 ***	0,000125 ***	0,000125 ***
iCSR	0,000125 ***	0,000250 ***	0,004499 **	0,000125 ***	0,000125 ***
LGCP	0,002500 **	0,238720	0,036995 *	0,147357	0,033996 *
iLGCP	0,000750 ***	0,026997 *	0,107737	0,093113 .	0,021372 *

VALIDATION

	B	D	K	L	N	O
CSR	0,000125 ***	0,000125 ***	0,000125 ***	0,000125 ***	0,000125 ***	0,000125 ***
iCSR	0,000125 ***	0,000125 ***	0,000125 ***	0,000125 ***	0,000125 ***	0,000250 ***
LGCP	0,521435	0,066742 .	0,008624 **	0,033621 *	0,004499 **	0,043745 *
iLGCP	0,000125 ***	0,009749 **	0,000125 ***	0,001500 **	0,000125 ***	0,245719

	P	S	t	U	X
CSR	0,000125 ***	0,000125 ***	0,000125 ***	0,000125 ***	0,000125 ***
iCSR	0,066742 .	0,000125 ***	0,000125 ***	0,002000 **	0,000125 ***
LGCP	0,002500 **	0,115486	0,032871 *	0,146732	0,021997 *
iLGCP	0,237970	0,000125 ***	0,041870 *	0,316585	0,000125 ***

Table S 1 Extreme rank envelope test p-values per sample area of the intensive dataset in calibration and validation, for the different models: completely spatial randomness (CSR); CSR with an inhomogeneous intensity (iCSR), log-Gaussian cox-processes (LGCP), LGCP with an inhomogeneous intensity (iLGCP). Significance codes: '***' for 0.001, '**' for 0.01, '*' for 0.05 and '.' for 0.1. Grey highlighting: highest p-value; bold blue: highest and non-significate p-value.

EXTENSIVE DATASET

CALIBRATION																
	A	B	C	D	E	F	G	H	I	J	K	L	M	N	O	R
CSR	6,66E-04	***	6,66E-04	***	6,66E-04	***	6,66E-04	***	6,66E-04	***	6,66E-04	***	6,66E-04	***	6,66E-04	***
iCSR	6,66E-04	***	6,66E-04	***	6,66E-04	***	6,66E-04	***	6,66E-04	***	6,66E-04	***	6,66E-04	***	6,66E-04	***
LGCP	2,94E-01		6,22E-01		2,11E-01		2,36E-01		2,74E-01		3,34E-01		3,11E-01		2,06E-01	
iLGCP	4,28E-01		7,44E-01		3,46E-02	*	3,66E-02	*	9,73E-02	.	9,45E-01		1,65E-01		1,83E-01	
CSR	6,66E-04	***	6,66E-04	***	6,66E-04	***	6,66E-04	***	6,66E-04	***	6,66E-04	***	6,66E-04	***	6,66E-04	***
iCSR	6,66E-04	***	6,66E-04	***	6,66E-04	***	6,66E-04	***	6,66E-04	***	6,66E-04	***	6,66E-04	***	6,66E-04	***
LGCP	3,42E-01		1,04E-01		2,66E-03	**	1,27E-02	*	3,75E-01		5,46E-02		1,49E-01		3,46E-02	*
iLGCP	3,86E-02	*	8,59E-02	.	5,33E-03	**	7,33E-03	**	5,66E-02	.	6,00E-03	**	2,81E-01		7,24E-04	***
CSR	6,66E-04	***	6,66E-04	***	6,66E-04	***	6,66E-04	***	6,66E-04	***	6,66E-04	***	6,66E-04	***	6,66E-04	***
iCSR	6,66E-04	***	6,66E-04	***	6,66E-04	***	6,66E-04	***	6,66E-04	***	6,66E-04	***	6,66E-04	***	6,66E-04	***
LGCP	1,07E-01		1,27E-02	*	2,03E-01		2,13E-02	*	2,66E-03	**	3,33E-03	**	3,13E-02	*	2,96E-01	
iLGCP	6,66E-04	***	3,33E-03	**	9,65E-01		6,66E-04	***	6,66E-04	***	6,66E-04	***	6,66E-04	***	4,66E-03	**
CSR	6,66E-04	***	6,66E-04	***	6,66E-04	***	6,66E-04	***	6,66E-04	***	6,66E-04	***	6,66E-04	***	6,66E-04	***
iCSR	6,66E-04	***	6,66E-04	***	6,66E-04	***	6,66E-04	***	6,66E-04	***	6,66E-04	***	6,66E-04	***	6,66E-04	***
LGCP	5,46E-02	.	2,66E-03	**	1,13E-02	*	2,66E-03	**	4,66E-03	**	2,13E-02	*	8,39E-02	.	2,71E-01	
iLGCP	3,33E-03	**	6,00E-03	**	6,66E-04	***	6,66E-04	***	6,66E-04	***	5,33E-03	**	3,33E-03	**	4,66E-03	**
CSR	6,66E-04	***	6,66E-04	***	6,66E-04	***	6,66E-04	***	6,66E-04	***	6,66E-04	***	6,66E-04	***	6,66E-04	***
iCSR	6,66E-04	***	6,66E-04	***	6,66E-04	***	6,66E-04	***	6,66E-04	***	6,66E-04	***	6,66E-04	***	6,66E-04	***
LGCP	2,93E-01		5,04E-01		6,46E-01		4,29E-01		5,26E-02	.	3,98E-01					
iLGCP	6,66E-04	***	5,66E-01		2,60E-02	*	3,60E-02	*	2,66E-03	**	1,41E-01					
VALIDATION																
	A	B	C	D	E	F	G	H	I	J	K	L	M	N	O	R
CSR	6,66E-04	***	6,66E-04	***	6,66E-04	***	6,66E-04	***	6,66E-04	***	6,66E-04	***	6,66E-04	***	6,66E-04	***
iCSR	6,66E-04	***	6,66E-04	***	6,66E-04	***	6,66E-04	***	6,66E-04	***	6,66E-04	***	6,66E-04	***	6,66E-04	***
LGCP	4,46E-02	*	5,19E-01		6,66E-01		1,67E-02	*	9,07E-01		4,60E-01		7,83E-01		2,00E-03	**
iLGCP	6,66E-04	***	7,57E-01		6,66E-04	***	6,66E-04	***	6,66E-04	***	5,46E-02	.	4,13E-02	*	6,66E-04	***
CSR	6,66E-04	***	6,66E-04	***	6,66E-04	***	6,66E-04	***	6,66E-04	***	6,66E-04	***	6,66E-04	***	6,66E-04	***
iCSR	6,66E-04	***	6,66E-04	***	6,66E-04	***	6,66E-04	***	6,66E-04	***	6,66E-04	***	6,66E-04	***	6,66E-04	***
LGCP	2,40E-02	*	1,33E-03	**	6,66E-04	***	6,66E-04	***	1,83E-01		6,66E-04	***	1,13E-01		6,66E-04	**
iLGCP	6,66E-04	***	6,66E-04	***	6,66E-04	***	6,66E-04	***	2,00E-03	**	6,66E-04	***	6,66E-04	***	6,66E-04	***
CSR	6,66E-04	***	6,66E-04	***	6,66E-04	***	6,66E-04	***	6,66E-04	***	6,66E-04	***	6,66E-04	***	6,66E-04	***
iCSR	6,66E-04	***	6,66E-04	***	6,66E-04	***	6,66E-04	***	6,66E-04	***	6,66E-04	***	6,66E-04	***	6,66E-04	***
LGCP	6,66E-04	***	6,66E-04	***	6,66E-04	***	6,66E-04	***	6,66E-04	***	6,66E-04	***	6,66E-04	***	1,33E-03	**
iLGCP	6,66E-04	***	6,66E-04	***	6,66E-04	***	6,66E-04	***	6,66E-04	***	6,66E-04	***	6,66E-04	***	6,66E-04	***
CSR	6,66E-04	***	6,66E-04	***	6,66E-04	***	6,66E-04	***	6,66E-04	***	6,66E-04	***	6,66E-04	***	6,66E-04	***
iCSR	6,66E-04	***	6,66E-04	***	6,66E-04	***	6,66E-04	***	6,66E-04	***	6,66E-04	***	6,66E-04	***	6,66E-04	***
LGCP	3,33E-03	**	6,66E-04	***	6,66E-04	***	6,66E-04	***	6,66E-04	***	6,66E-04	***	6,66E-04	***	1,13E-02	*
iLGCP	5,33E-03	**	6,66E-04	***	6,66E-04	***	6,66E-04	***	9,25E-04		6,66E-04	***	2,66E-03	**	2,00E-03	**
CSR	6,66E-04	***	6,66E-04	***	6,66E-04	***	6,66E-04	***	6,66E-04	***	6,66E-04	***	6,66E-04	***	6,66E-04	***
iCSR	6,66E-04	***	6,66E-04	***	6,66E-04	***	6,66E-04	***	6,66E-04	***	6,66E-04	***	6,66E-04	***	6,66E-04	***
LGCP	6,66E-04	***	1,33E-03	**	4,53E-01		6,66E-04	***	6,66E-04	***	6,66E-04	***	6,66E-04	***	6,66E-04	***
iLGCP	6,66E-04	***	6,66E-04	***	6,66E-04	***	6,66E-04	***	6,66E-04	***	6,66E-04	***	2,04E-01			

Table S 2 Extreme rank envelope test p-values per sample area of the extensive dataset in calibration and validation, for the different models: completely spatial randomness (CSR); CSR with an inhomogeneous intensity (iCSR), log-Gaussian cox-processes (LGCP), LGCP with an inhomogeneous intensity (iLGCP). Significance codes: '*' for 0.001, '**' for 0.01, '*' for 0.05 and '.' for 0.1. Grey highlighting: highest p-value; bold blue: highest and non-significate p-value.**

Intensive dataset

	σ^2	α	Intercept (β_0)	Hpop (β_1)	Crop (β_2)	Tree (β_3)	Remot (β_4)	Hpop ² (β_5)	Crop ² (β_6)	Tree ² (β_7)	Remot ² (β_8)
B	3,25E+00	4,19E+03	-1,78E+01	-6,71E-01	2,85E-02	2,36E-02	4,41E-03	9,16E-02	-3,00E-04	-5,66E-04	-1,82E-05
D	1,78E+00	7,61E+03	-1,87E+01	7,83E+00	3,03E-02	1,40E-03	-3,56E-03	-6,70E+00	-4,01E-04	-1,69E-05	1,16E-06
K	2,70E+00	5,24E+03	-1,77E+01	4,57E+00	-4,16E-03	3,60E-02	-6,13E-03	-4,32E+00	1,74E-04	-1,57E-03	3,77E-06
L	1,65E+00	1,15E+04	-1,81E+01	4,05E+00	2,81E-02	2,16E-03	2,86E-03	-3,01E+00	-3,75E-04	-1,74E-04	-1,08E-05
N	2,90E+00	3,17E+03	-2,04E+01	4,87E+00	4,90E-02	5,06E-02	2,82E-04	-2,96E+00	-3,77E-04	-1,22E-03	-7,26E-07
O	2,33E+00	6,28E+03	-1,79E+01	5,62E+00	-2,90E-02	-3,54E-03	-3,20E-03	-4,61E+00	3,62E-04	-3,25E-04	1,23E-06
P	2,80E+00	7,31E+03	-1,95E+01	7,82E+00	1,61E-04	8,34E-02	-7,52E-03	-6,66E+00	-1,82E-05	-4,07E-03	6,12E-06
S	4,11E+00	3,74E+03	-1,93E+01	5,48E+00	5,46E-02	-4,55E-03	-1,60E-03	-4,51E+00	-8,01E-04	-5,45E-05	-4,75E-06
t	1,93E+00	2,07E+04	-2,26E+01	1,23E+01	2,54E-02	3,16E-02	9,53E-04	-9,14E+00	-2,24E-04	-3,89E-04	-1,52E-07
U	3,50E+00	8,94E+03	-1,92E+01	1,15E+01	-4,02E-03	-7,25E-02	3,13E-03	-1,20E+01	-9,72E-05	9,78E-04	-4,87E-05
X	2,83E+00	5,61E+03	-1,94E+01	1,13E+01	-1,33E-02	1,76E-02	-4,84E-03	-1,01E+01	2,41E-04	-2,67E-04	2,77E-06

Extensive dataset

	σ^2	α	Intercept (β_0)	Hpop (β_1)	Crop (β_2)	Tree (β_3)	Remot (β_4)	Hpop ² (β_5)	Crop ² (β_6)	Tree ² (β_7)	Remot ² (β_8)
A	8,44E-01	3,24E+03	-1,33E+01	3,40E+00	-2,06E-03	-2,54E-02	1,12E-03	-2,50E+00	1,12E-04	2,68E-04	-3,30E-06
B	7,50E-01	7,11E+03	-1,47E+01	9,56E+00	-2,03E-02	2,04E-02	-1,42E-04	-8,04E+00	3,72E-04	-2,44E-04	2,37E-07
C	6,63E-01	3,08E+03	-1,38E+01	5,84E+00	1,22E-02	-1,04E-02	1,34E-03	-3,71E+00	-9,64E-05	3,23E-05	-1,93E-06
D	9,86E-01	3,31E+03	-1,38E+01	7,70E+00	-2,32E-03	1,39E-02	-8,73E-05	-5,83E+00	7,87E-05	-1,65E-04	-3,17E-07
E	8,53E-01	1,59E+03	-1,27E+01	6,89E+00	-2,55E-05	-7,87E-03	-2,03E-05	-4,51E+00	3,74E-05	2,39E-05	-6,32E-07
F	6,48E-01	1,04E+04	-1,68E+01	9,80E+00	1,19E-02	1,88E-02	4,72E-03	-6,64E+00	-6,25E-05	-1,42E-04	-2,59E-06
G	1,02E+00	1,82E+03	-1,29E+01	5,60E+00	7,97E-03	-2,37E-02	-1,33E-03	-3,23E+00	-1,03E-04	1,89E-04	1,38E-07
H	9,66E-01	2,32E+03	-1,35E+01	6,12E+00	1,17E-02	-5,79E-03	7,73E-04	-3,19E+00	-1,77E-04	-5,23E-06	-9,98E-07
I	1,24E+00	2,38E+03	-1,46E+01	1,32E+01	1,97E-02	1,78E-02	7,73E-04	-1,56E+01	-1,92E-04	-2,17E-04	-7,50E-07
J	8,36E-01	2,54E+03	-1,36E+01	6,85E+00	-6,93E-04	-1,66E-03	-1,42E-03	-5,52E+00	6,35E-05	8,67E-05	8,66E-07
K	6,13E-01	2,01E+03	-1,26E+01	2,46E+00	-1,63E-04	-1,19E-02	-4,45E-04	-1,34E+00	2,84E-05	1,19E-04	-1,77E-06
L	7,60E-01	3,26E+03	-1,24E+01	4,43E+00	-1,03E-03	-1,07E-02	-4,45E-03	-2,85E+00	3,09E-05	7,72E-05	5,71E-06
M	1,42E+00	2,90E+03	-1,41E+01	6,71E+00	-4,96E-03	-6,01E-03	-1,14E-04	-6,36E+00	1,21E-04	-6,34E-05	-2,42E-07
N	6,92E-01	2,33E+03	-1,35E+01	4,20E+00	3,65E-03	-1,55E-02	-4,72E-04	-2,90E+00	-2,09E-05	1,81E-04	-9,92E-07
O	7,86E-01	3,90E+03	-1,37E+01	7,14E+00	-1,19E-02	-7,09E-03	3,57E-04	-4,67E+00	1,83E-04	7,44E-06	-7,16E-07
R	5,38E-01	2,33E+03	-1,31E+01	6,86E+00	1,52E-02	-5,01E-03	-1,82E-03	-5,17E+00	-1,67E-04	4,15E-05	3,49E-07
S	1,01E+00	2,90E+03	-1,53E+01	1,11E+01	-1,02E-02	3,25E-03	9,36E-04	-1,05E+01	1,46E-04	-2,09E-04	-9,11E-07
t	7,30E-01	3,95E+03	-1,39E+01	4,16E+00	9,50E-03	-2,05E-03	-2,61E-04	-3,33E+00	-5,65E-05	-2,32E-04	-7,23E-07
U	8,74E-01	2,28E+03	-1,35E+01	6,44E+00	-9,06E-03	-1,63E-02	-3,24E-04	-5,25E+00	1,17E-04	1,05E-04	-5,52E-07
V	6,20E-01	1,94E+03	-1,30E+01	5,24E+00	-2,31E-03	-2,48E-02	-6,63E-04	-2,91E+00	9,26E-05	3,03E-04	-8,49E-07
W	7,42E-05	2,11E+02	-1,26E+01	5,70E+00	8,37E-04	-1,24E-02	1,63E-03	-4,86E+00	1,69E-05	2,27E-04	-5,76E-06
X	1,02E-05	2,47E+02	-1,27E+01	4,47E+00	-2,63E-03	-2,13E-03	2,40E-03	-2,84E+00	8,64E-05	-4,48E-05	-5,78E-06
Y	4,43E-01	4,20E+03	-1,38E+01	7,07E+00	-3,82E-03	-2,95E-02	1,33E-03	-5,55E+00	1,36E-04	4,81E-04	-4,27E-06
Z	5,67E-01	1,11E+04	-1,71E+01	2,05E+01	1,85E-02	-2,57E-03	2,26E-03	-4,53E+01	-1,52E-04	-1,03E-04	-1,42E-06
AA	5,20E-01	3,12E+03	-1,34E+01	4,67E+00	-6,11E-03	9,22E-03	-1,15E-03	-3,46E+00	1,09E-04	-1,95E-04	-7,13E-08
AB	9,92E-01	2,51E+03	-1,34E+01	3,31E+00	3,08E-03	4,36E-03	1,11E-03	-1,85E+00	1,53E-05	-1,99E-04	-2,43E-06
AC	8,31E-01	9,28E+02	-1,26E+01	4,25E+00	1,14E-02	-6,59E-03	-1,75E-03	-2,50E+00	-1,13E-04	-6,98E-05	2,85E-06
AD	3,82E-06	2,30E+02	-1,25E+01	4,68E+00	1,40E-02	8,39E-04	-5,35E-04	-3,05E+00	-1,46E-04	-1,00E-04	1,23E-06
AE	1,69E-06	2,30E+02	-1,30E+01	5,04E+00	3,69E-03	-1,33E-02	1,88E-03	-3,54E+00	3,84E-05	3,97E-05	-3,61E-06
AG	5,58E-01	7,47E+03	-1,37E+01	3,43E+00	2,17E-02	-2,16E-03	-3,67E-03	-2,22E+00	-2,01E-04	-7,06E-05	4,17E-06
AH	9,21E-01	7,44E+03	-1,35E+01	1,64E+00	1,39E-02	1,06E-02	2,99E-03	-1,00E+00	-1,19E-04	-2,26E-04	-5,47E-06
AI	8,54E-01	4,27E+03	-1,33E+01	4,47E+00	-1,06E-03	-1,41E-02	-1,61E-03	-2,67E+00	1,42E-05	4,22E-05	3,69E-07
AJ	2,06E+00	1,10E+04	-1,80E+01	6,92E+00	2,40E-02	3,41E-02	5,03E-03	-3,84E+00	-1,08E-05	-3,48E-04	-3,89E-06
AK	1,25E+00	3,17E+03	-1,36E+01	2,69E+00	1,66E-02	-1,72E-02	-1,04E-03	-1,43E+00	-2,15E-04	1,71E-04	1,50E-06
AM	8,22E-01	1,99E+03	-1,30E+01	4,99E+00	1,79E-02	8,50E-04	-3,40E-03	-3,28E+00	-2,73E-04	9,29E-06	1,47E-06
AN	9,44E-01	2,79E+03	-1,35E+01	4,48E+00	6,27E-03	8,65E-03	-1,92E-03	-2,19E+00	-9,27E-05	-1,08E-04	1,60E-07
AO	5,93E-01	3,63E+03	-1,32E+01	4,67E+00	2,69E-02	-1,13E-02	-1,33E-03	-3,11E+00	-2,37E-04	3,19E-05	-4,95E-07
AQ	1,17E+00	5,66E+03	-1,29E+01	3,27E+00	1,43E-02	-1,18E-02	-5,58E-03	-2,17E+00	-1,79E-04	2,07E-04	2,94E-06

Table S 3 Coefficients of the different model parameters (α , σ^2 and $\beta_0, \beta_1 \dots \beta_8$). In LGCP models, the covariance is defined as $C_0(r) = \sigma^2 \exp(r/\alpha)$ where σ^2 is the variance and α the scale parameter and the intensity function was defined as $\lambda(u) = \exp(\beta_0 + \beta_1 Hpop(u) + \beta_2 Crop(u) + \beta_3 Tree(u) + \beta_4 Remot(u) + \beta_5 Hpop^2(u) + \beta_6 Crop^2(u) + \beta_7 Tree^2(u) + \beta_8 Remot^2(u))$.

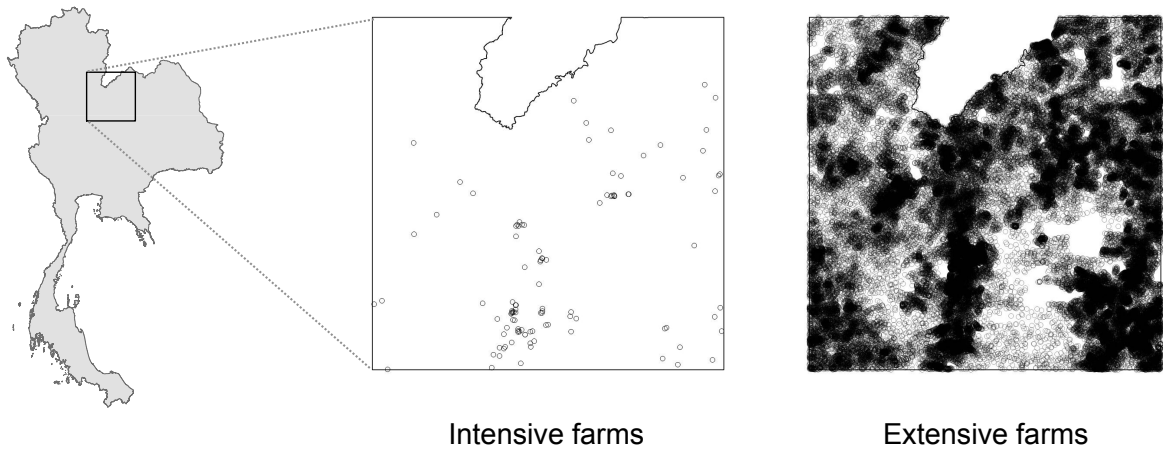


Figure S 6. Intensive and extensive observed distribution of farms in a sample area.